

SPUTTERING OF THIN FILM RESISTORS

by

Myron Jan Peterson

A Thesis Submitted to the Faculty of the
DEPARTMENT OF ELECTRICAL ENGINEERING
In Partial Fulfillment of the Requirements
For the Degree of
MASTER OF SCIENCE
In the Graduate College
THE UNIVERSITY OF ARIZONA

1 9 6 9

STATEMENT BY AUTHOR

This thesis has been submitted in partial fulfillment of requirements for an advanced degree at The University of Arizona and is deposited in the University Library to be made available to borrowers under rules of the Library.

Brief quotations from this thesis are allowable without special permission, provided that accurate acknowledgment of source is made. Requests for permission for extended quotation from or reproduction of this manuscript in whole or in part may be granted by the head of the major department or the Dean of the Graduate College when in his judgment the proposed use of the material is in the interests of scholarship. In all other instances, however, permission must be obtained from the author.

SIGNED: *Myron J. Peterson*

APPROVAL BY THESIS DIRECTOR

This thesis has been approved on the date shown below:

Ray H. Mattson

R. H. Mattson

Professor of Electrical Engineering

1-10-69

Date

ACKNOWLEDGMENTS

The author wishes to thank the personnel of the Solid State Engineering Laboratory of The University of Arizona for their unstinting assistance and advice during the fabrication processes. In particular, the author wishes to thank his advisor, Dr. Roy H. Mattson, and Mr. Victor A. Wells for their advice and guidance during the preparation of this thesis and Mrs. Freida H. Long for her efforts in preparation of the manuscript.

TABLE OF CONTENTS

	Page
LIST OF ILLUSTRATIONS	v
ABSTRACT	vii
Chapter 1 INTRODUCTION	1
Chapter 2 SPUTTERING THEORY	4
Chapter 3 EQUIPMENT AND MATERIALS USED	15
SP 210 A Module	15
Power Supply Unit	20
Vacuum System	22
Materials	23
Chapter 4 D.C. AND R.F. SPUTTERING RESULTS	24
Anticipated Results	26
Choice of Standard Values and Limits of Change	28
Nichrome Results	30
Fused Quartz Results	40
Nickel, Molybdenum and Tantalum Results	42
General Observation	52
Processing Compatibility	53
Chapter 5 HYBRID RESISTOR AND CAPACITOR FABRICATION RESULTS	55
Resistor Results	58
Capacitor Results	59
Chapter 6 CONCLUSIONS	61
Appendix A SPUTTERED THIN FILM DEPOSITION PROCEDURE	63
Appendix B ETCHING PROCEDURES	65
REFERENCES	69

LIST OF ILLUSTRATIONS

Figure		Page
1	Diode Sputtering Configuration	5
2	Mean Free Path vs. Pressure	7
3	Triode Sputtering Configuration	9
4	Action of Radio Frequency Probe	14
5	R. D. Mathis Module	16
6	Probes for R.F. and D.C. Sputtering	19
7	Control Panel	21
8	Arrangement of Microscope Slide on Substrate Platform	25
9	Deposition Thickness vs. Time for Nichrome and Fused Quartz	31
10	Deposition Thickness vs. Pressure for Nichrome and Fused Quartz	33
11	Deposition Thickness vs. Anode Current for Nichrome and Fused Quartz	34
12	Deposition Thickness vs. Target Voltage for Nichrome (D.C. voltage) and Fused Quartz (R.F. voltage)	36
13	Deposition Thickness vs. Magnetic Field Current for Nichrome and Fused Quartz	37
14	Ohms/square Resistance vs. Thickness for Nichrome	39
15	Deposition Thickness vs. Time for Nickel, Molybdenum and Tantalum	43
16	Deposition Thickness vs. Pressure for Nickel, Molybdenum and Tantalum	45
17	Deposition Thickness vs. Anode Current for Nickel, Molybdenum and Tantalum	46

List of Illustrations (Continued)

Figure		Page
18	Deposition Thickness vs. Target Voltage for Nickel, Molybdenum and Tantalum	47
19	Deposition Thickness vs. Magnetic Field Current for Nickel and Tantalum	49
20	Sheet Resistance vs. Thickness for Nickel, Molybdenum and Tantalum	50
21	Mask	57
22a	Thin Film on Substrate with Etched Channel	66
22b	Thin Film on Substrate with Reflective Aluminum Film for Thickness Measurements	66

ABSTRACT

This work deals with the process of sputtering thin films suitable for use with monolithic integrated circuits. The thin films are subsequently formed into circuits elements by photoengraving processes.

In order to obtain repeatable results, the sputtering module is first characterized by varying each of several independent rate-effecting parameters over a limited range while observing the resulting variations in film thickness. Optimum parameter settings are thus developed. Using these results, thin films of the desired thickness and sheet resistance were sputtered. Then compatible photoengraving processes were developed to form resistors, capacitors and passivating insulators. The processes used for sputtering and photoengraving are explained, and the resistor and capacitor test results are presented.

Chapter 1

INTRODUCTION

Physical sputtering which once was considered a nuisance phenomenon has become a useful technique for producing thin film depositions required in integrated circuit processing. In the most general form physical sputtering is defined as the ejection of atoms from a target source under the influence of ion bombardment. The ejected atoms form the resulting thin film [Seeman, 1965].

The sputtering phenomenon was first observed by W. R. Grove in 1852 [Nickerson and Moseson, 1965], but only in the early 1900's were adequate theories for the sputtering process formulated by Langmuir and Guentersulze. A century after being observed, the first thin films were intentionally sputtered for a few specific electronic and research applications. During the 1950's Wehner developed more versatile methods of sputtering and advanced the theoretical investigation of the phenomenon.

As a result of Wehner's investigations, a renewed interest developed in the sputtering of thin films. This interest was largely due to the need for carefully controlled thin film depositions to be used with integrated and hybrid electronic circuits. Thin films are used in integrated circuits to provide interconnections for the diffused elements as well as bonding pads. Insulating sputtered thin films can

be used as a passivation layer for integrated circuits and metallic films as circuit elements in hybrid integrated circuits.

There are many advantages of sputtered thin film over evaporated thin films which is the other major technique for film production. Evaporative techniques require undesirably high deposition rates to minimize interaction between the evaporant and the residual gases present at the substrate surface. The greater control of sputtered films provides reproducible tolerances of $\pm 5\%$ [Nickerson and Moseson, 1964]. The sputtered atom has better adhesion since its average energy of 10 to 30 electron volts is an order of magnitude higher than that of an evaporated atom. Alloys of almost any proportion can be sputtered and, in this manner, the temperature coefficients of resistive films can be readily controlled. Sputtering allows for the deposition of four categories of thin films: resistors, conductors, semiconductors, and dielectrics. Evaporative techniques allow deposition of metals and only a few dielectrics such as SiO and SiO_2 . Accurate control of these few dielectrics is difficult to obtain by evaporative techniques. Reasonably priced evaporative systems introduce film contamination by the use of boats, filaments or crucibles which are not present in sputtering systems. Thus, the versatility and control allowed when sputtering makes it appealing for the deposition of circuit elements as well as simple interconnections for integrated circuits.

This thesis will be concerned with the sputtering of thin film resistors, capacitors, and distributed elements, as well as the compatibility of these elements with integrated circuit processing. Several

metals will be investigated for use as resistors and distributed resistor-capacitors. Fused quartz will be investigated as a dielectric material for use in capacitors and distributed resistor-capacitors. Processing compatibility with diffused devices will be observed for all of the materials used.

The sputtering process will first be reviewed starting with the theory of D.C. diode sputtering. From D.C. diode sputtering, the theory will be logically expanded to include D.C. triode sputtering, reactive sputtering and R.F. sputtering. After the theory of sputtering is reviewed, the equipment and materials used in sputtering experiments will be explained. Next, the experimental results such as the deposition rates obtained when changing the control parameters are presented. Comparisons of observed results to anticipated results are made. The control variables are time, pressure, anode current, target voltage, magnetic field current and substrate temperature. They will be varied during the experiments.

The ultimate goal of the experiments is twofold. First, information about the specific deposition rates for various materials as sputtered in the R. D. Mathis module is discussed. Second, useful nichrome resistors and nichrome-SiO₂-aluminum capacitors are to be realized.

Chapter 2

SPUTTERING THEORY

The basic sputtering mechanism depends on the fact that an ion bombarded target material ejects atoms which are then deposited as a thin film on all the surrounding surfaces. D.C. diode sputtering uses a simple cold cathode target material and an anode biased to a high positive potential in a vacuum (Fig. 1). After an initial pump-down to pressure less than 10^{-6} torr, an inert gas like argon is used to back fill the system. The pressure is allowed to increase to about 10^{-2} to 10^{-1} torr. At this pressure electrons emitted from the cathode collide with the argon molecules causing ionization of some of the argon. The resulting positive ions are attracted to the negative-biased cathode-target where they embed themselves in the target material. Atoms of the target material are ejected by one of three simultaneous mechanisms momentum transfer which is the dominant mechanism, local high temperature spots, and volatile chemical formation.

In the momentum transfer process, the incident ion penetrates the target material and suffers a series of collisions with atoms of the target material. In order to eject a surface atom, the incident ion must suffer collisions such that its vector is reversed and then its momentum is transferred to a surface atom. Studies indicate that this collision process occurs in the first four atomic layers [Wolsky, 1966].

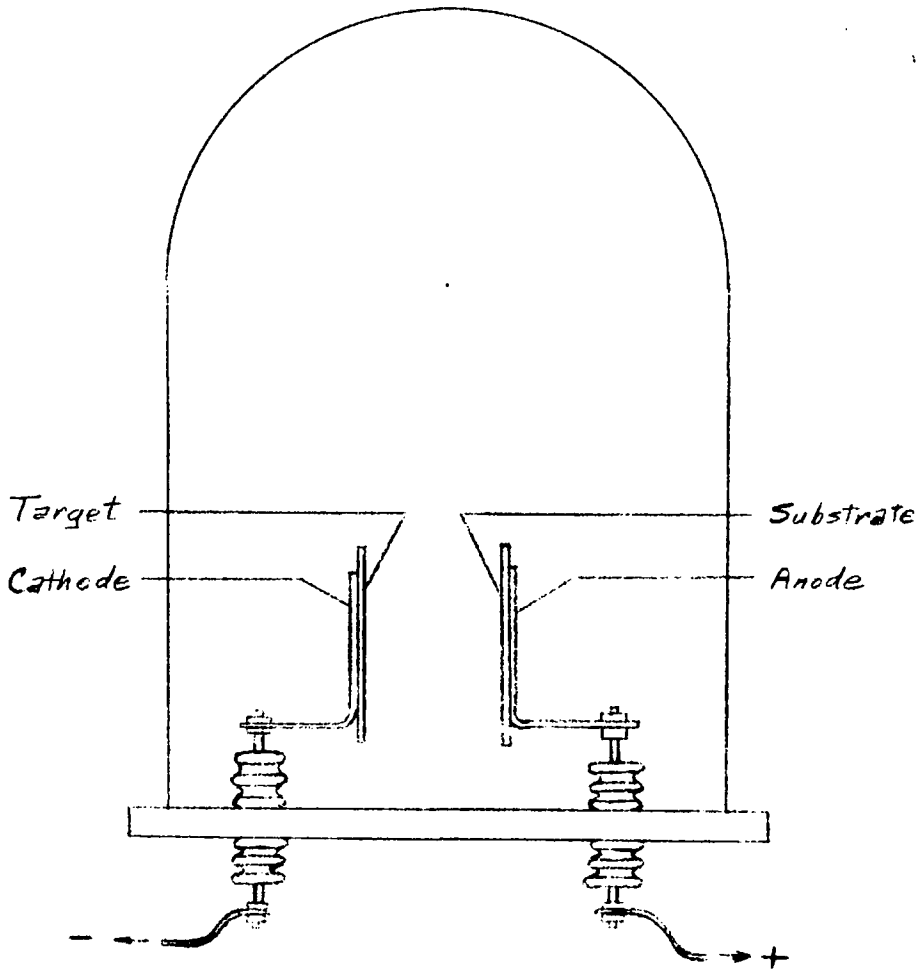


Fig. 1 Diode Sputtering Configuration

The local high temperature mechanism occurs when the impinging ion transfers energy to the sputtered surface causing a rapid temperature rise in a small region of atomic dimensions. Local volatilization of the surface material results in the ejection of the surface atoms.

The volatile chemical mechanism is associated with the formation of compounds on the target surface. These compounds are volatile at normal temperatures and decompose in the presence of the glow discharge. This process should not be confused with that of reactive sputtering which will be described in detail later in the chapter [Blevins, 1964].

The ejected target atoms travel in straight lines in all directions until they are deposited on a surrounding surface as a thin film. The substrates on which it is desired to have the target material deposited are attached to the anode. The anode is generally in a plane parallel to that of the cathode-target. A major limitation of diode sputtering is that sustaining the argon plasma discharge requires relatively high pressure (10^{-2} to 10^{-1} torr). The plasma is dependent on the cathode emitted electrons producing more than one argon ion electron pair enroute to the anode. High pressure is necessary to achieve multi-ion generation. At this high pressure the mean free path of the target atom is small (about 2 cm.) therefore requiring a small target to substrate spacing. By having the target to substrate distance less than the atom mean free path, the majority of the ejected atoms will reach the substrate without suffering collisions (Fig. 2).

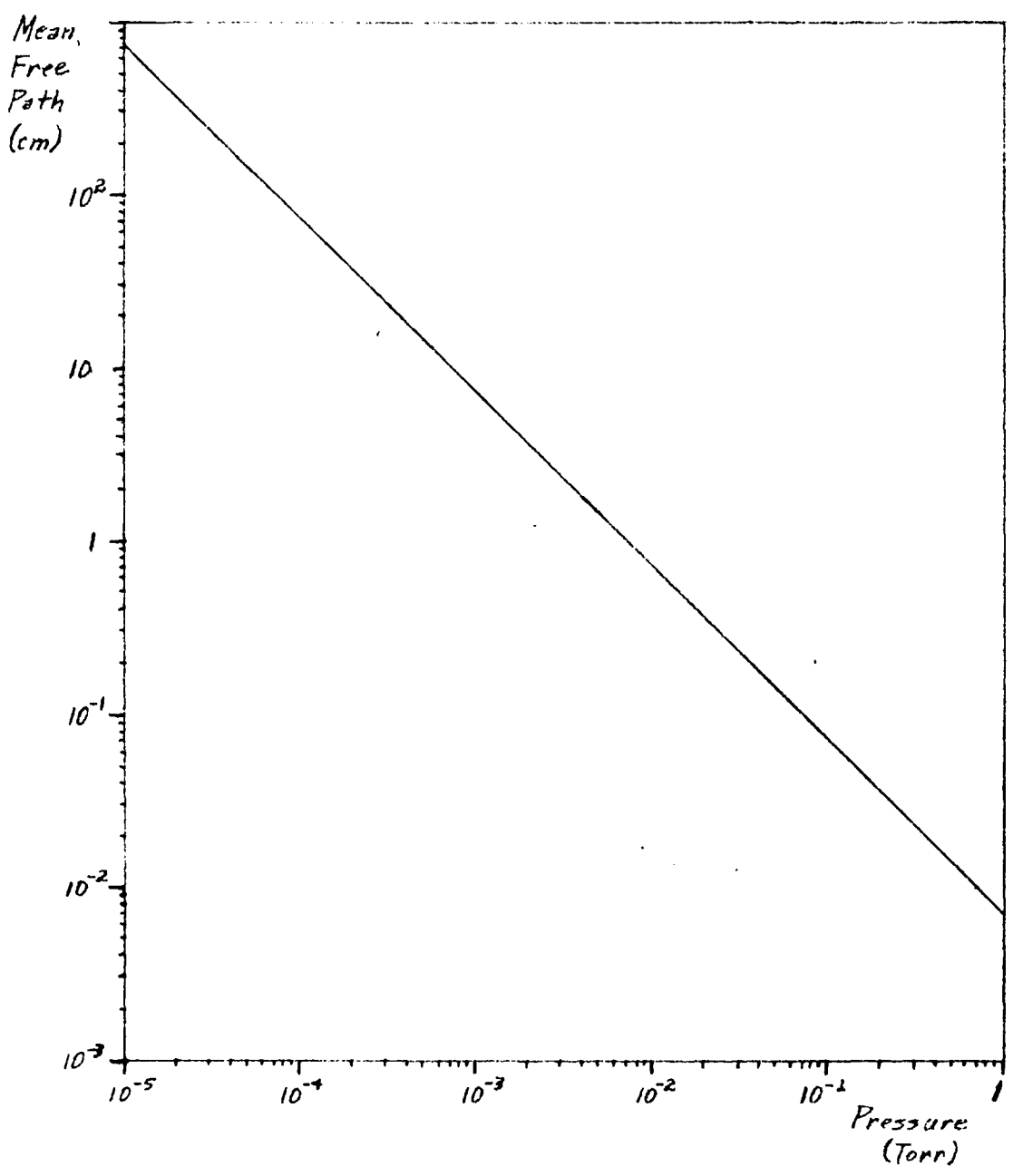


Fig. 2 Mean Free Path vs. Pressure

This high pressure problem can be overcome by the more versatile triode sputtering configuration (Fig. 3). The R. D. Mathis SP 210A module used in the Solid State Engineering Laboratory (SSEL) is of the triode type. The triode configuration has a thermionic emission cathode (a hot tungsten filament) which supplies electrons to ionize the argon gas. These electrons are attracted to the positively biased (about 100 volts) anode but suffer collisions with the argon gas enroute. If the electron has sufficient energy, it will give up part of its energy in an inelastic collision with the argon producing either an excited molecule or an ion and an extra electron. Both the original electron and the one from the ionized argon then continue toward the anode possibly suffering further collisions enroute. In this triode case, avalanche effect may result but it is not essential to sustain the plasma. The cathode is a source of electrons which will sustain the plasma. If the electrons have insufficient energy, they will scatter elastically without appreciable energy loss (less than 2%), and a plasma will not be generated. The argon ions, electrons and neutral argon atoms form a gas plasma which is electrically neutral. The plasma is typified by a luminous pinkish-violet glow. Since the hot cathode supplies many electrons to sustain the plasma, much lower operating pressures (down to 2×10^{-4} torr) are used than in the diode case. The resulting mean free path increases to about 10 cm. at 5×10^{-4} torr, thus allowing greater target-substrate distances (Fig. 2). Instead of the cathode being the target, in triode sputtering a Langmuir probe faced with the target material is inserted near the side of the gas plasma and is biased from

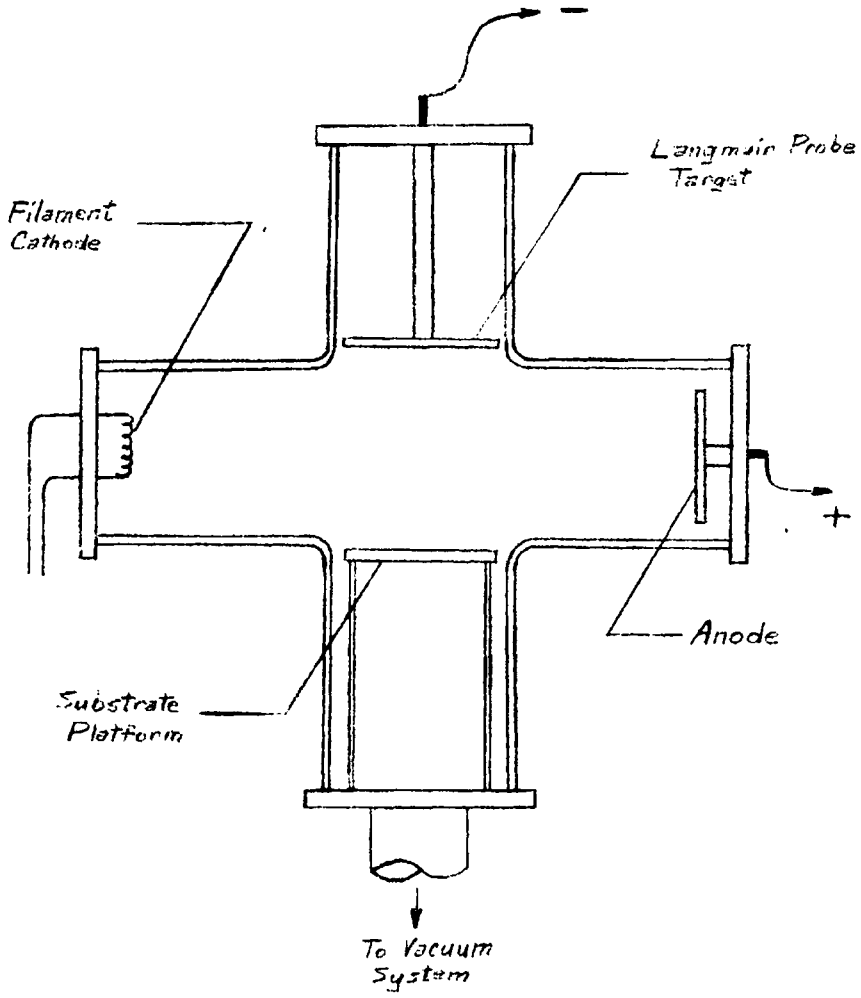


Fig. 3 Triode Sputtering Configuration

several hundred to several thousand volts negative. This highly biased probe attracts positive ions from the plasma. This causes sputtering of the target probe. Momentum transfer is the dominant sputtering mechanism. The substrate which will be covered with target atoms, is located opposite and generally parallel to the target material and is usually electrically isolated from the rest of the circuitry.

When the substrate is electrically connected into the circuit, bias sputtering results. Bias sputtering is useful particularly when removing impurities from the deposited film during deposition. Film contamination occurs because of the gettering action between fresh metallic films and chemical active residual gases in the vacuum chamber [Seeman, 1966]. A small negative bias on the sputtered substrate causes it, as well as the target, to be sputtered by ionic bombardment. But the substrate bias is much less than that of the target, thus a net deposition occurs on the substrate. This back sputtering of the substrate is preferential and loosely bound impurities are removed from the film.

Vratny and Harrington have found that residual oxygen causes the major degradation of the resistance of deposited films [Hall, 1967]. The preferential removal of oxygen by back sputtering in tantalum films is associated with two factors, the collision cross-section area of oxygen versus tantalum and the sputtering thresholds of the two materials. The collision cross-section area of oxygen is 5.45 times that of tantalum. Thus, the probability of an oxygen ion collision is much higher than a tantalum ion collision assuming equal densities of tantalum and oxygen impurity atoms.

The sputtering threshold of tantalum is 25 to 30 ev. with some observed threshold values as high as 100 ev. while the sputtering threshold of oxygen is only 9 ev. These effects are reflected in calculations by Vratny and Harrington [1965] which show that argon is 4.25 times as productive in sputtering oxygen atoms as tantalum atoms. But this cited reference also concludes from comparison of these calculations and actual observed effects of residual oxygen that this theory of ion bombardment alone is insufficient to explain the observed results. Thus, they suggest that two other mechanisms may be present. The first of these is argon incorporation into the film which doesn't clean the film, but increases film resistance. The second is a cleaning process associated with the presence of a high electron flux near the substrate during half of the asymmetric sputtering cycle. This process is not fully understood at present although it has been observed by Peterman [1963], Redhead [1964], and Moore [1961].

Another type of sputtering, reactive sputtering, occurs when a reactive gas such as O_2 , CO , or N_2 is present in the sputtering module. Usually this reactive gas is mixed in the desired amount with argon before being used to back fill the sputtering module. In reactive sputtering three distinct steps are present:

- 1) sputtering of neutral atoms from the target by ionic bombardment and transit of these atoms toward the substrate,
- 2) generation of negative ions over the substrate, and
- 3) reaction of the sputtered target atoms with the negative ions.

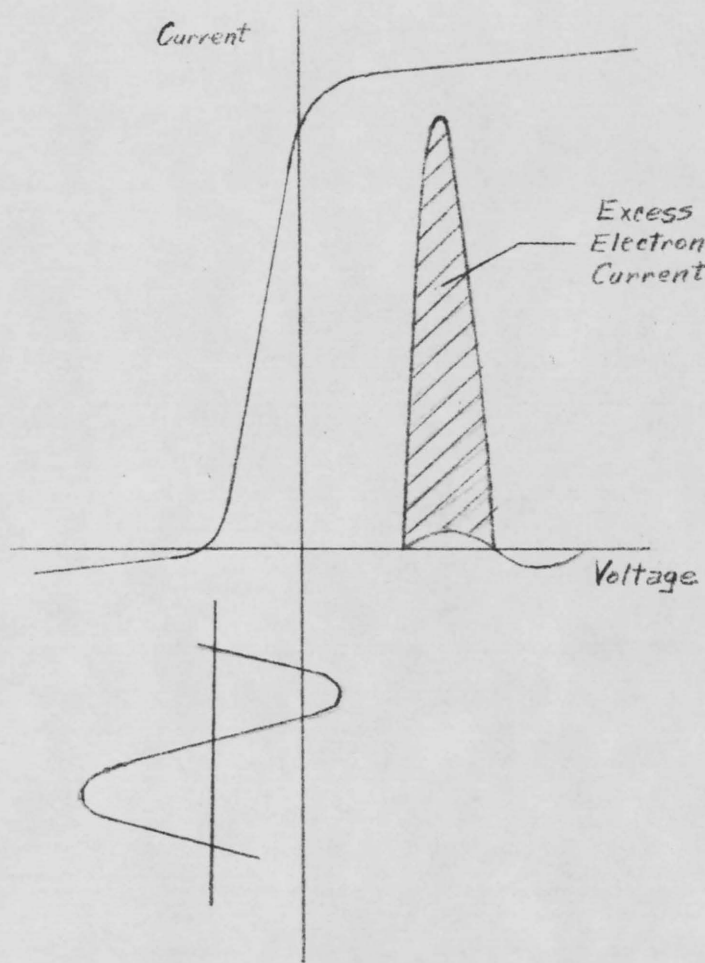
Reactive sputtering of the target material occurs as previously explained with the momentum transfer mechanism being the dominant source of the sputtered atoms. Negative ions are generated in the plasma by the dissociation of neutral molecules in the gas discharge. This is followed by either ionization, recombination or charge exchange, and by electron attachment to molecules having a strong affinity for electrons. The negative ions have a low mobility and form a sheath near the positive biased substrate (or anode in diode sputtering). The sputtered target atoms react with these negative ions enroute from the target to the substrate causing combination prior to deposition. By controlling the reactive gas being mixed with argon, properties of the resultant film can be altered to vary resistance and temperature coefficients.

Because reactive sputtering requires higher pressures to reduce the mean free path to less than the target-substrate distance, diode sputtering becomes a very practical configuration for that case. As discussed, only conducting materials can be used effectively with D.C. sputtering, but even insulators can be sputtered using radio frequency (R.F.) sputtering which will now be discussed.

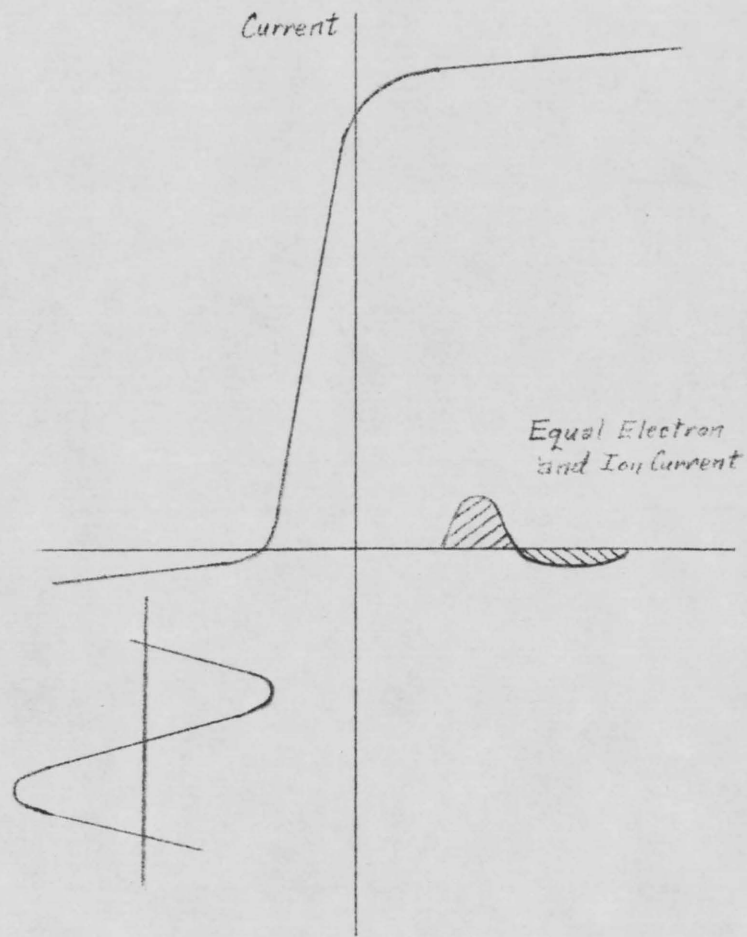
If an insulating face is used on the Langmuir probe and a pre-insulating shield enclosing the back part of the probe, no net D.C. current can flow from the probe with reasonable D.C. potentials applied. Then a positive charge builds up on the probe face. This positive charge opposes the ion bombardment causing the sputtering action. However, when an R.F. potential is applied, a large electron current will be drawn to the probe during the first half of the cycle due to the high

mobility of electrons (Fig. 4a). During the second half cycle, a positive ion current will be drawn but less charge will be transferred because of the lower ion mobility. Thus, a new displacement charge builds up on the probe face until after many cycles an equilibrium condition is reached as the electron current equals the ion current (Fig. 4b). Once equilibrium is reached, the ion current flows for considerably more than half the total R.F. cycle to compensate for the peaked nature of the highly mobile electron current flow.

The R.F. swing about a new negative potential causes a variation in the bombarding ion energy dependent on the R.F. peak potential and on the R.F. frequency. For frequencies below 10 megacycles the energy spread will be appreciable but fortunately, it is of secondary importance, since a detailed knowledge of the energy is not necessary in film preparation. The R. D. Mathis module used in the SSEL experiments has both D.C. and R.F. sputtering capabilities as well as limited bias and reactive sputtering capabilities.



A. When First Turned On



B. After Equilibrium Is Reached

Fig. 4 Action of Radio Frequency Probe [Blevis, 1964]

Chapter 3

EQUIPMENT AND MATERIALS USED

Investigation of sputtered thin films was conducted using the R. D. Mathis SP 210 A triode sputtering module (Fig. 5). It was mounted on a National Research Corporation six-inch diffusion pump vacuum system capable of an ultimate pressure of 3×10^{-7} torr.

SP 210 A Module

The SP 210 A module is composed of a 6" x 4" pyrex pipe cross having a width of 26" and a height of 30" which includes a 4" base feed through ring. The electron source is from either of two 50 turn, 10 mil, hot tungsten filaments located in one end of the 4" pyrex cross arm. A variac controls the filament current: 6.4 amps was used throughout the experimental work. This was experimentally determined to provide sufficient electrons to form the plasma at about 9×10^{-4} torr and maintain it to 2×10^{-4} torr. The use of low current in each filament prolongs its life. The dual filament features allows switching from one to the other in case of filament failure during an experiment. External fins on the aluminum filament housing and a high velocity fan provide adequate cooling for dissipating a filament power of approximately 250 watts.

The anode is located in the opposite end of the 4" pyrex cross arm and is also provided with a finned aluminum housing and a high velocity cooling fan. The weight of the anode housing balances that of the filament housing so that the module can rest stably on a flat surface.

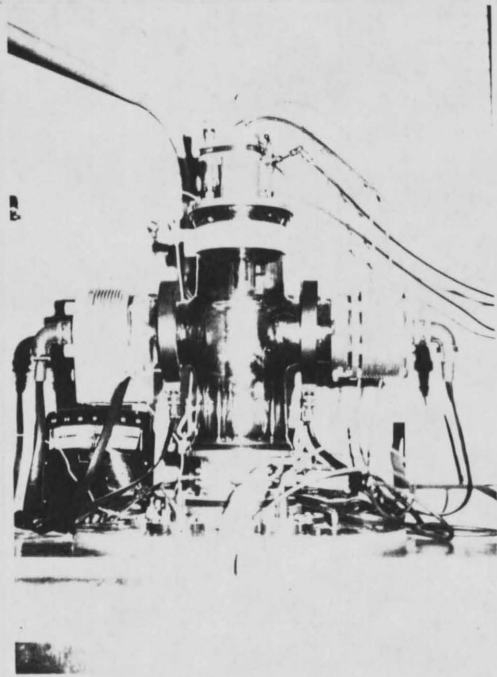


Fig. 5 R. D. Mathis Module

The 6" diameter top of the pyrex cross is closed with a top plate which holds the target probe and provides the target biasing and water cooling feed throughs. The top plate has a Vacronic Vari-vac VV 500 micrometer valve fitted to allow back-filling of the system with an inert or reactive gas mixture. A dry nitrogen venting valve allows the system to return to atmospheric pressure upon completion of an experimental run.

The D.C. target probe is a 5" copper disc supported from the top plate by a large copper tube. Cooling water tubing is fed through the support tube to the back surface of the copper probe where it is soldered. This provides target cooling (Fig. 6a). A glass protective layer surrounds the tube and the rear of the target disc to prevent sputtering from the back of the probe. Electrical bias is supplied through the center wire of a coaxial led from the power supply which is connected to the copper tube supporting the target probe. Electrical isolation from the water pipes in the building, which may be grounded, is provided by two lengths of tygon tubing approximately four feet long attached to the water feed throughs in the top plate.

Target materials can be mounted to the probe by any of four methods:

- 1) Heavy gauge stock can be attached by hard soldering or silver soldering a 6-32 machine screw stud to the center of the stock. The stud is then screwed into the 6-32 tapped hole in the center of the probe.

2) Thin gauge stock and foils can be attached using the three threaded holes spaced around the probe periphery. Small tabs of the target material must be placed under the screws and folded back covering the screw heads to prevent sputtering of the screw material along with the target material.

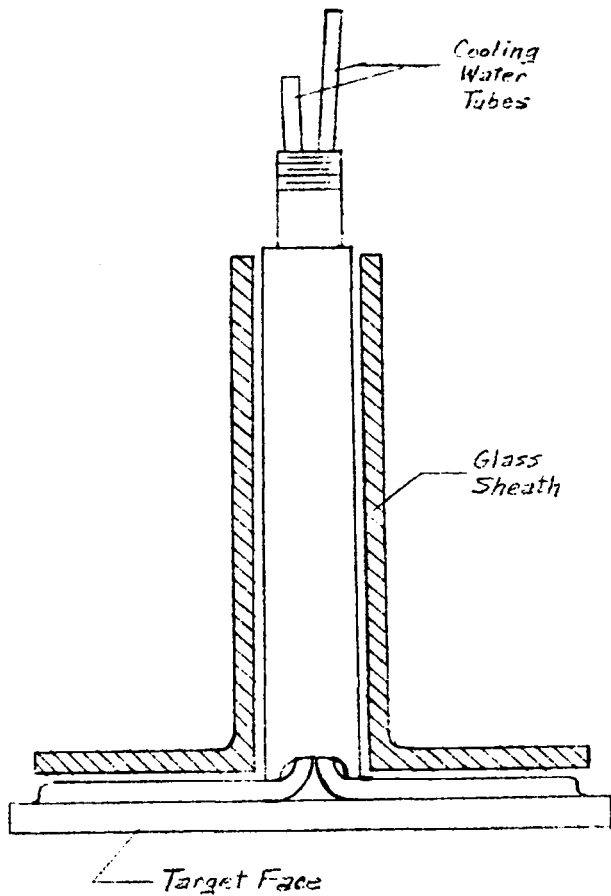
3) The probe itself can be electroplated with the target material or a copper disc with a center stud attached can be electroplated and drawn up tight against the probe.

4) Brittle materials such as quartz, pyrex, or cermets can be attached to a copper disc using a conductive epoxy cement. The copper disc with a 6-32 machine screw stud soldered to its reverse side is then screwed to the probe.

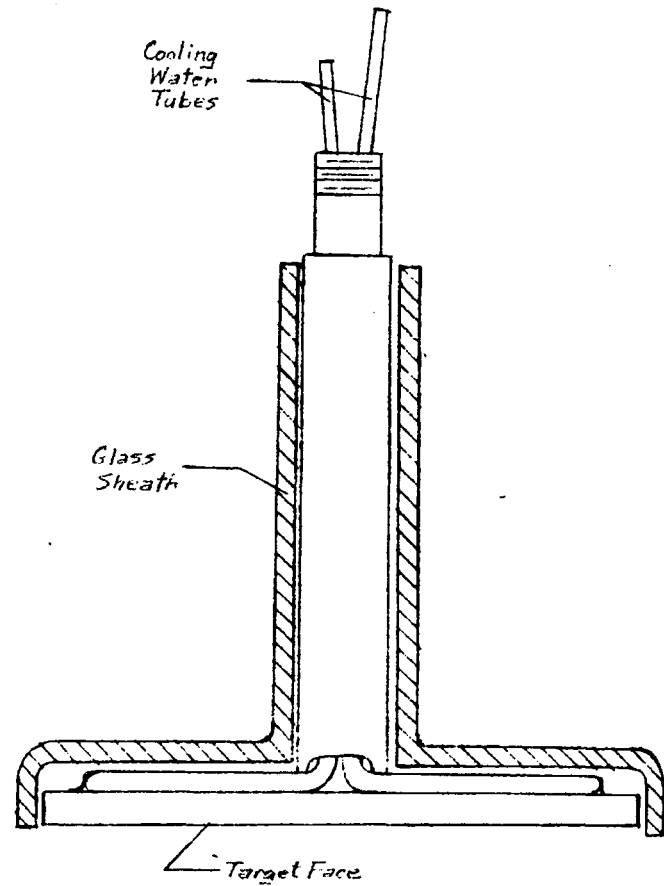
To improve the thermal conductivity, vacuum grease was applied between the probe face and the back surface of the target material since better sputtering results when the probe is kept at a constant temperature. All target materials were cut at least 1/2" larger than the probe diameter to prevent sputtering from the edges of the copper probe.

The R.F. probe, a smaller 4" diameter disc, is also supported by a copper tube (Fig. 6b). Water cooling is provided similar to the D.C. probe but the glass sheath in this case extends completely around the edges of the probe. It is ground flat to fit snugly against the rear surface of the material to be sputtered.

A copper table is attached to the base feed through ring and the 6" pyrex cross fits snugly around the table. This substrate platform has coils for water cooling and a disc heating element for substrate



A. D.C. Probe



B. R.F. Probe

Fig. 6 Probes for R.F. and D.C. Sputtering

heating. The platform was allowed to float electrically in all of the experiments conducted. Electrical isolation from the water system is again provided by tygon tubing. An iron-constantan thermocouple monitored the temperature of the back surface of the substrate material through a small hole drilled in the substrate platform.

Control of the plasma density and thus the sputtering rate is provided by a magnetic field. The magnetic field is produced by two coils, one on each horizontal arm of the pyrex cross. The coils can easily produce a field of 100 ampere turns. A 2 ampere current through the coils produces a 20 gauss magnetic field in the center of the plasma region directly over the center of the substrate platform.

Power Supply Unit

The power supply for the module contains filament, low voltage anode, high voltage probe, radio frequency, and magnetic field power supplies. The controls are interlocked to prevent improper turn-on sequence or operation without cooling fans. The control panel also includes metering for the filament current, anode current, D.C. target voltage and current, magnetic field current, radio frequency volt voltage and current, and filament selection (Fig. 7).

A single 300 volt-amp center tapped transformer and a variac form the filament supply which can provide up to 8.0 amps of current through the filament. The anode power is provided by a 200 volt, 4 ampere solid state bridge rectified supply with a capacitor filter. Anode currents up to 3 amperes were available although a maximum current of

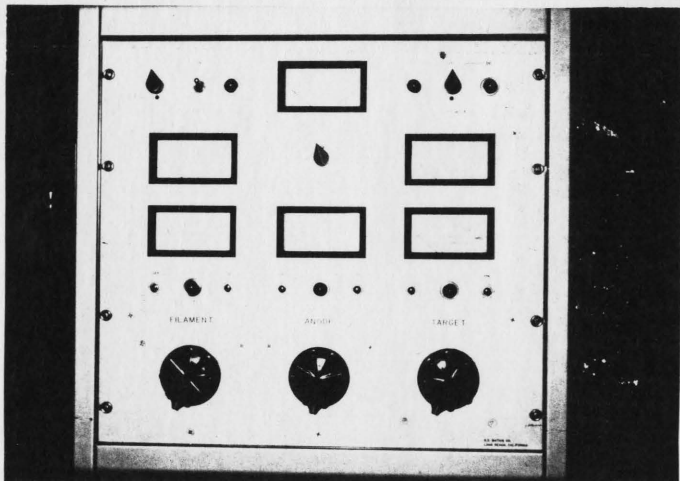


Fig. 7 Control Panel

2.5 amperes was used due to indications that parts of the power supply were overheating.

A dual purpose high voltage supply provides a negative target probe voltage for D.C. sputtering of a high voltage to the R.F. unit when R.F. sputtering was used. The maximum D.C. potential available is 3.0 kilovolts although the highest bias used in the experiments was 2.5 kilovolts.

The choice between the R.F. and D.C. mode of sputtering is made by a console panel switch. The R.F. generator consists of a crystal controlled 100 kc oscillator and a 500 watt class C amplifier. Amplifier-target probe coupling is made through a series inductance to compensate for the capacitive load of the probe. This results in maximum power transfer.

Vacuum System

The SP 210 module was mounted on an NRC 6" diffusion pump system using two adaptor plates with O-ring seals. The 6" diffusion pump is capable of an ultimate pressure of 3×10^{-7} torr with the module using chilled water trapping. Pump down from atmosphere required about 2 hours to reach a pressure of about 5×10^{-7} torr. At pressures above 1×10^{-6} torr, sufficient residual gases are left to affect the film properties in an unpredictable manner. Oxygen trapping in the film was the principal problem. It generally increases the sheet resistance of the film. A Welch type NRC 6 D mechanical roughing foreline pump having a nominal capacity of 6.75 cubic feet per minute was used. Foreline pressures below 40 microns (4×10^{-2} torr) were maintained for all experiments.

Pressure gauging is provided by two thermocouple type gauges, one in the base ring of the module and the second in the foreline, and by an ion gauge, NCR type 507 (Bayard-Alpert type). The thermocouple and ion gauge tubes are controlled by a single NRC Model 510 B controller which allows individual balancing of the thermocouple gauges, adjustment of the emission current, and outgassing of the ion gauge tube.

The thermocouple used to monitor the temperature on the backside of the substrate is connected to a Honeywell Model 105 R 12 Pyn-O-Volt temperature controller. The controller could be set to turn the substrate heater on and off at any desired temperature up to about 250°C while continuously indicating the substrate temperature. The temperature variation for a 205°C setting on the controller was between 195°C and 210°C with 2 amps at 114 volts being applied to the heater. A monitor of the heater voltage and current and a voltage variac control were located on the NRC control console.

Materials

Argon was used in all of the sputtering experiments since it is inexpensive and readily available. Any of the other inert gases (helium, neon, krypton, xenon, or radon) could also be used for non-reactive sputtering. Sputtering rate could be expected to increase with increasing atomic numbers as the sputtering rate is a function of the weight of the bombarding ion used.

The D.C. sputtering was conducted using nickel, nichrome (80% nickel, 20% chrome), tantalum and molybdenum. The R.F. sputtering used only fused quartz for resistor passivation and capacitor dielectrics.

Chapter 4

D.C. AND R.F. SPUTTERING RESULTS

This chapter is initiated by indicating the expected results caused by changing sputtering parameters. The standard settings used and their high and low limits are presented, and the reasons for the choice of the standard settings are given. Last to be presented in this section are the observed results in deposition thickness caused by changing sputtering time, anode current, magnetic field current, target voltage, module pressure, and substrate temperature. Included are possible explanations of any variation from the anticipated results.

The step-by-step procedure for operation of the sputtering module is found in Appendix A. Appendix B provides the step-by-step procedure used in photoetching of both thickness measurement slides and the silicon wafers used in capacitor and resistor design.

The materials studied were nickel, nichrome, molybdenum, tantalum, and fused quartz. In order to produce useful data, five values of each of six variables were arbitrarily selected for measuring purposes. These extended across the range of control allowed by the R. D. Mathis SP 210 A module and its control console. As one variable was changed between its limits, each of the other five were held constant. The depositions were made on 1x3 inch precleaned glass microscope slides placed on the substrate platform (Fig. 8). The depositions were later measured for thickness using the method explained in Appendix B. The

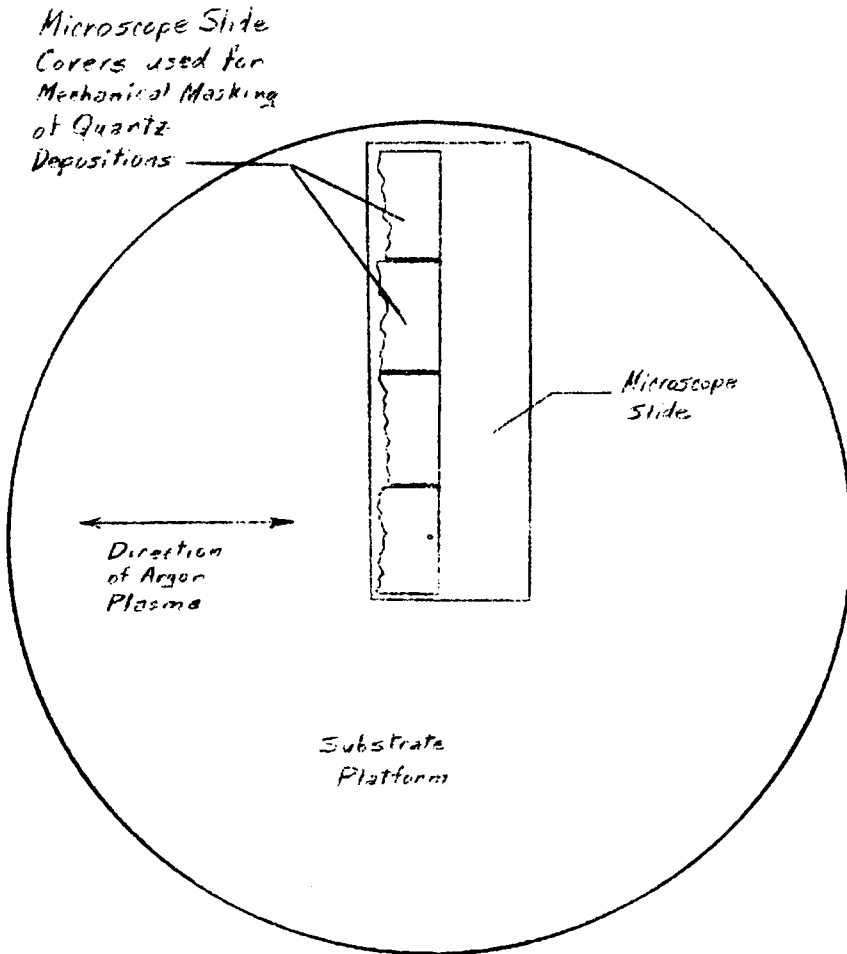


Fig. 8 Arrangement of Microscope Slide on Substrate Platform

depositions for resistors and capacitors were sputtered onto a silicon dioxide layer on silicon wafers. The silicon wafers were placed in the center of the substrate platform.

Anticipated Results

The following predictions were theoretically anticipated as a result of changing the various sputtering parameters. As time is increased, the deposition thickness should increase linearly with time. Some variation can be expected during the initial position of the deposition period. Oxides formed during the cycling of the vacuum system to atmospheric pressures, can be expected to have a slightly different sputtering rate than the pure target material.

The effect of pressure is related to the density of the plasma formed at that pressure. At lower pressures fewer atoms are available to be ionized so a less dense plasma would be formed. Thus, as plasma density decreases, sputtering rate should also decrease.

A decrease in plasma density can also be caused by lowering the anode voltage as indicated by the anode current monitored. Less anode voltage (and thus current) decreases the energy with which the electrons strike the argon. This lowers the ionization yield of electrons which in turn reduces the number of ions in the gas plasma. Increasing the anode voltage increases the yield until virtually all of the argon atoms are ionized. Further increases have little effect on the plasma density. Thus, deposition thickness should vary in a similar manner with anode voltage.

The target voltage determines the number and energy of the bombarding argon atoms from the gas plasma. Therefore, as target voltage is decreased, fewer ions are attracted and the bombarding energy is lessened which decreases the sputtering rate. Increased target voltage has the opposite effect but the effect saturates when most of the bombarding atoms have the energy necessary to ensure sputtering of the target material.

Presence of a magnetic field parallel to the desired plasma axis causes electrons not on the centerline between the filament and anode to spiral toward the centerline. This increases the plasma density near the centerline. This focusing of the plasma density along the centerline will cause higher sputtering rates over the center of the substrates but decreased sputtering rates toward the edges of the substrate platform. Thus, the uniformity of the depositions can be expected to vary more over the entire substrate platform when a magnetic field is present. This is acceptable if only a small portion of the substrate platform near the center is used during the deposition.

Substrate temperature can be expected to have little effect on the deposition rate. However, it may significantly effect the form of crystalline growth and therefore the properties of the sputtered film.

Filament current, which is an indication of the number of electrons available for ionization, can be expected to effect the plasma density greatly. Filament current, however, was not used as a variable as filament life was deemed more important for these experiments.

Choice of Standard Values and Limits of Change

A time of one hour was chosen as the standard deposition time. The effects of target oxidation on deposition thickness are minimized by using such a relatively long sputtering time. Most oxidation that might occur is removed in the first fifteen minutes of sputtering. Furthermore thickness measurements are more easily made on the thicker films produced by longer sputtering times. When time was the varied parameter, fifteen minutes was the shortest time used and 75 minutes the longest. With time held constant at one hour, pressure was the next parameter to be varied.

The standard pressure used for the sputtering runs was 7×10^{-4} torr. This was a midscale pressure with the lowest being 2×10^{-4} torr and the highest pressure being 2×10^{-3} torr. The plasma would extinguish when the pressure dropped to 1×10^{-4} torr. Thus, the lower limit of 2×10^{-4} torr was necessary to maintain the plasma. At pressures higher than 2×10^{-3} torr the vacuum system foreline pressure rose rapidly above 60 microns. This limited operation of the system to pressures of 2×10^{-3} torr or less.

The next parameter to be varied was anode current. An anode current of 1.5 amperes was used as the midscale standard current. This correlated to an anode voltage of 80 to 90 volts from filament to anode. The lowest current used was 0.5 amperes as less current caused the plasma to collapse. A maximum of 2.5 amperes was used as this was near the maximum available from the console control.

Target bias voltage was the next parameter varied. The midscale reading of 1.5 kilovolts was chosen as the standard setting. The lower limit used was 0.5 kilovolts although the target bias voltage could be decreased to zero. An upper limit of 2.5 kilovolts was used as this approached the maximum available from the control console.

Magnetic field current was varied as the next parameter. A value of 1.8 amperes was chosen as the standard value. This value seemed to produce the highest plasma density over the center of the substrate platform. This corresponds to 13.5 gauss over the center of the substrate. The validity of this choice for the maximum density was verified by the experimental results (Fig. 13). No magnetic field current was used as the minimum and 2.0 amperes as the maximum. This 1000 ampere-turn maximum produced a 14.0 gauss magnetic field over the center of the substrate platform.

The last parameter to be varied was substrate temperature. The temperature was allowed to rise from about 30°C to 50°C during the deposition cycle for the standard setting. This rise was due to the energy of the sputtered atoms deposited on the substrate. The literature indicates that a uniform temperature is more important to obtain uniform film properties than is the actual temperature of the substrate. The lower temperature limit obtained by chilled water cooling of the substrate platform was 20°C. A maximum substrate temperature of 200°C was used as the upper limit of the heating element was found to be around 230°C.

Other parameters which were not varied were filament current, ionic precleaning time, and substrate biasing. The filament current was maintained at 6.4 amperes for all depositions. This was found to be the lowest value consistently able to fire and maintain the gas plasma. A low value is desirable to prolong filament lifetime. Ionic cleaning of the target and substrate was used on all runs before actual sputtering was commenced. The ionic cleaning was accomplished by forming the gas plasma and allowing ionic bombardment scrubbing of both target and substrate before any bias was applied to the target. Five minutes of this ionic cleaning were used before each deposition. No substrate biasing was used in any of the sputtering runs as the substrate was allowed to float electrically.

Nichrome Results

This section describes the results obtained when sputtering nichrome. Time of deposition was changed as the first variable with the other variables being set on their respective standard settings. These settings were: pressure - 7×10^{-4} , anode current - 1.5 amperes, target voltage - 1.5 kilovolts, magnetic field current - 1.8 amperes, and substrate temperature at commencement of each run - 30°C . Time intervals of fifteen minutes were used starting with fifteen minutes and ending with 75 minutes. As expected, a nearly linearly increasing deposition thickness resulted as time was increased (Fig. 9). The experimental results indicated that the initial deposition rate was $56 \text{ \AA}/\text{minute}$ but dropped to $40 \text{ \AA}/\text{minute}$ within 30 minutes. This indicates that any oxide that was formed on the nichrome target surface tends to sputter

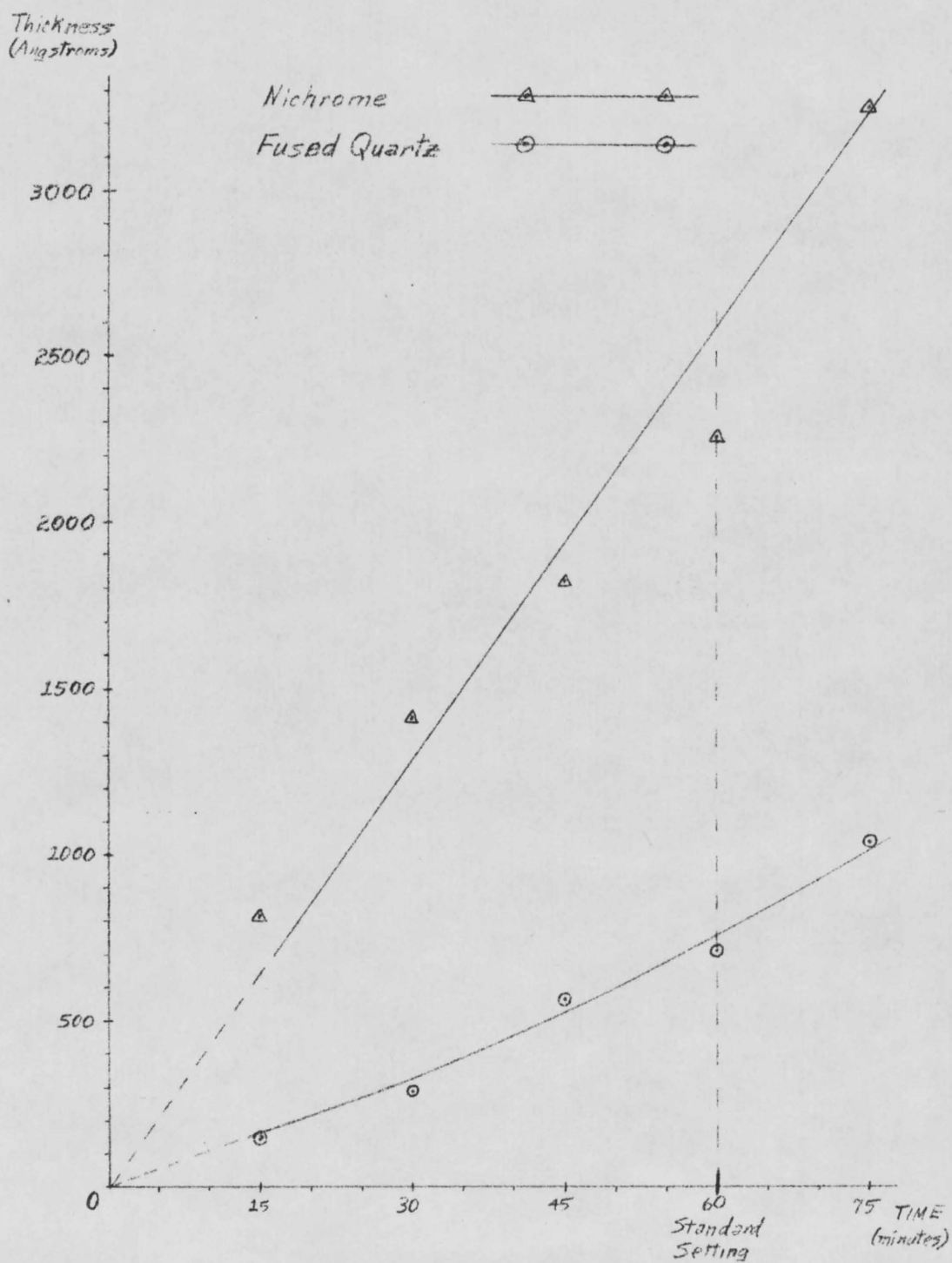


Fig. 9 Deposition Thickness vs. Time for Nichrome and Fused Quartz

more rapidly than the pure nichrome which is exposed after about 15 to 30 minutes of sputtering action.

Pressure was the next controlled variable. The other parameter standard settings were: time - 60 minutes, anode current - 1.5 amperes, target voltage - 1.5 kilovolts, magnetic field current - 1.8 amperes, and initial substrate temperature - 30°C. The five values of pressure used were 2×10^{-4} torr, 5×10^{-4} torr, 7×10^{-4} torr, 1×10^{-3} torr, and 2×10^{-3} torr. Surprisingly, the lowest pressure produced the highest sputtering rate of 55 Å/minute (Fig. 10). A possible explanation of this unexpected result is that the increased plasma density due to higher pressure caused backspattering from the substrate.

The next variable changed was anode current induced by changing the anode voltage. The current was varied from 0.5 amperes to 2.5 amperes in 0.5 ampere steps. Standard settings for the other parameters were: time - 60 minutes, pressure - 7×10^{-4} torr, target voltage - 1.5 kilovolts, magnetic field current - 1.8 amperes, and initial substrate temperature - 30°C. Increasing anode current caused higher sputtering rates (Fig. 11). This is as expected as the increased current caused more complete ionization within the plasma, thus a more dense source of bombarding ions for the target.

Target voltage was the next variable changed. Target voltages from 500 volts to 2500 volts in 500 volt increments were used. The standard settings for the other variables were: time - 60 minutes, pressure - 7×10^{-4} torr, anode current - 1.5 amperes, magnetic field current - 1.8 amperes, and initial substrate temperature - 30°C. As

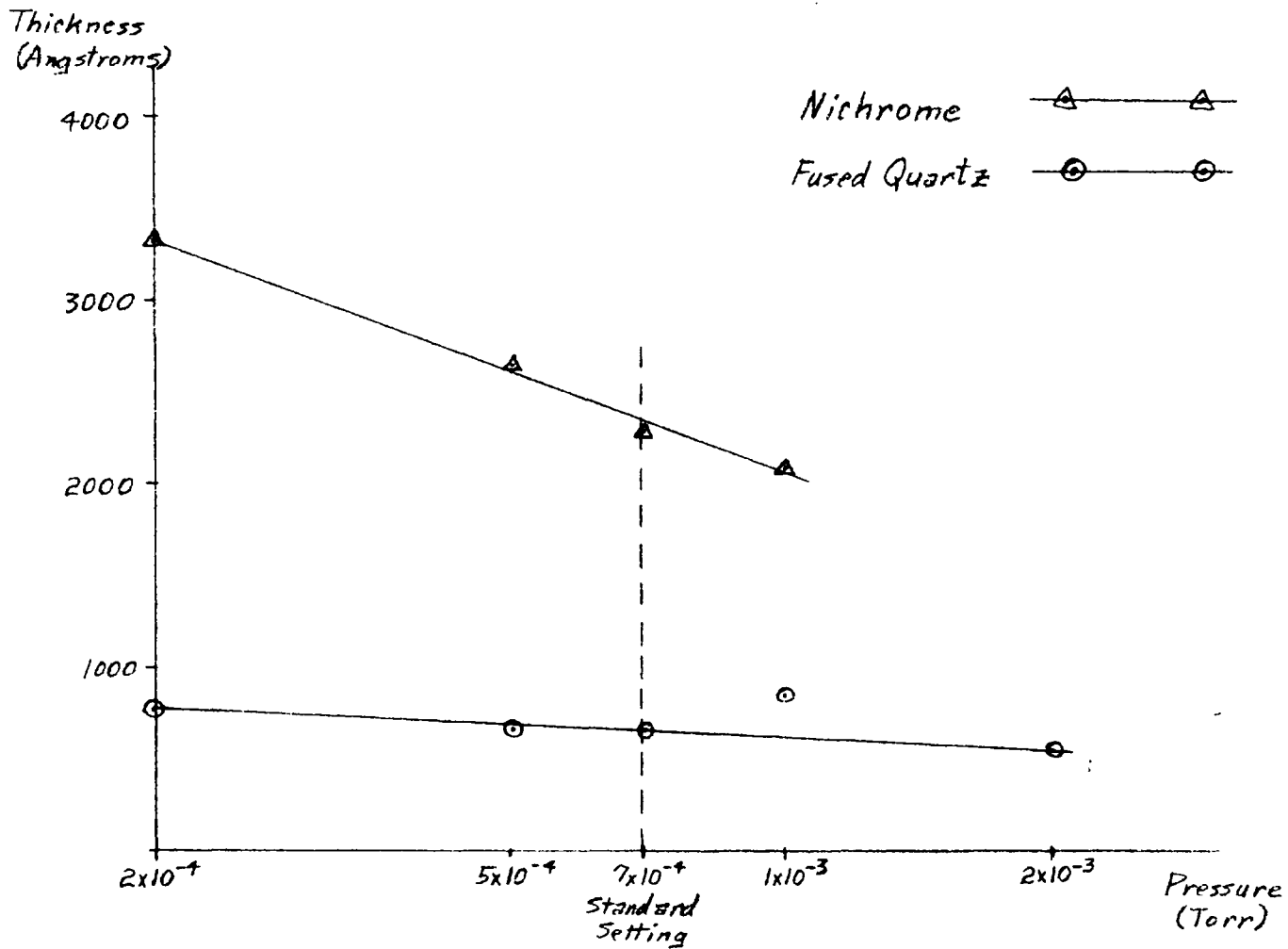


Fig. 10 Deposition Thickness vs. Pressure for Nichrome and Fused Quartz

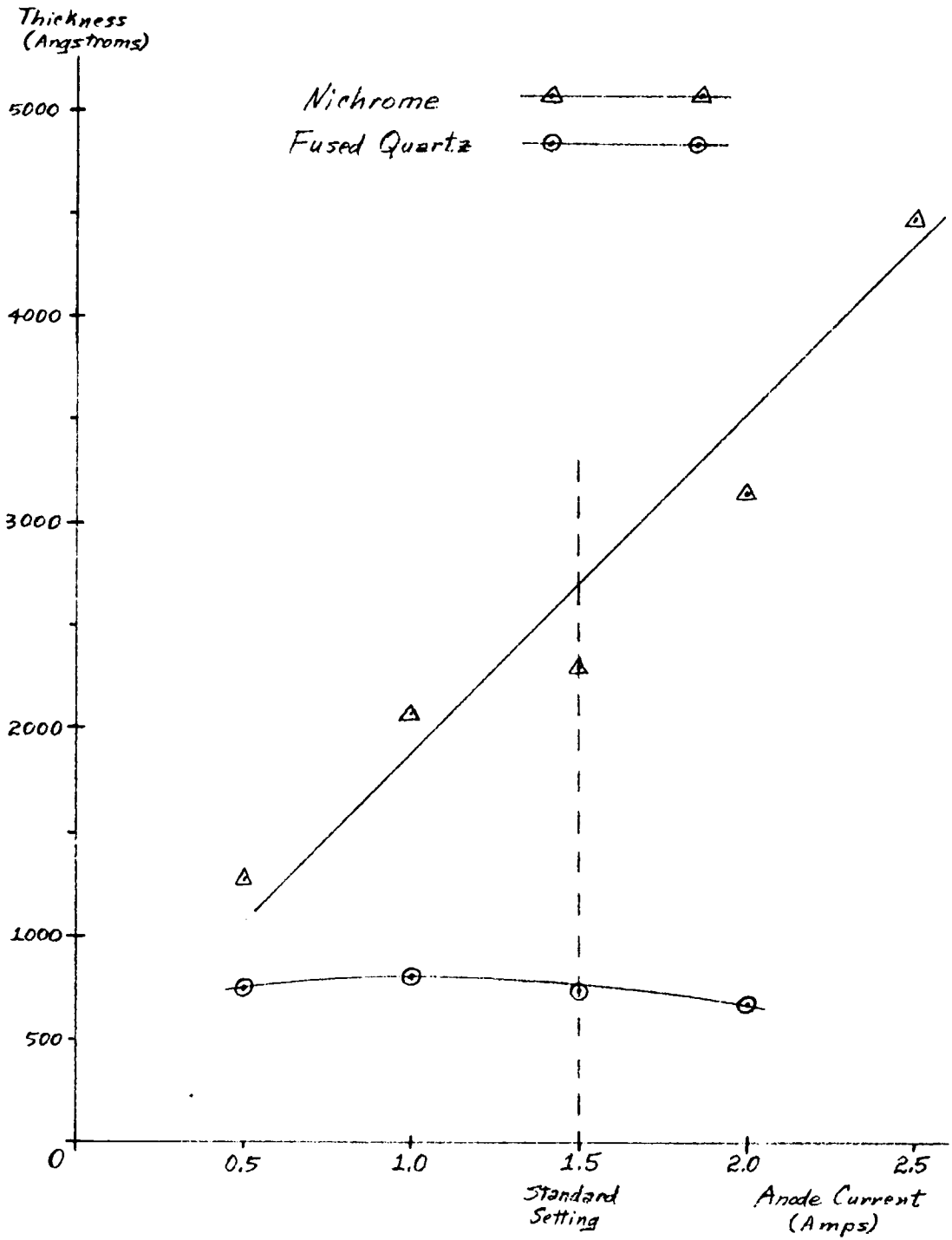


Fig. 11 Deposition Thickness vs. Anode Current for Nichrome and Fused Quartz

target voltage increased, the sputtering rate also increased (Fig. 12). The rate increase tended toward a maximum value which was beyond the maximum permitted by the control console. This is expected since large changes in target voltage are necessary to produce small increases in sputtering yield once most of the bombarding ions have sufficient energy to produce sputtering.

The next variable to be changed was magnetic field intensity. This was indicated by changes in the current flow to the magnetic coils. The current flow was varied from no current, thus no magnetic field to 2.0 amperes in 0.5 ampere increments. The standard settings for the other variables were: Time - 60 minutes, pressure - 7×10^{-4} torr, anode current - 1.5 amperes, target voltage - 1.5 kilovolts, and initial substrate temperature - 30°C . As magnetic current flow increased from 0 to 1.5 amperes, an accompanying increase in deposition rate occurred (Fig. 13). After a peak corresponding to 1.5 amperes, the deposition rate then dropped off with further increases in magnetic field current. A possible explanation is that the greatly increased density of the plasma over the centerline caused collisions with the sputtered atoms in this central region which reduced the number that reached the substrate without being deflected.

The last variable to be changed was the substrate temperature. The results of changing substrate temperature were inconclusive and suggested that substrate temperature changes from 20°C to 200°C had little effect on deposition rate. No measurements were made of other possible effects due to different substrate temperatures. One such probable change would be in the crystalline structure of the deposited film.

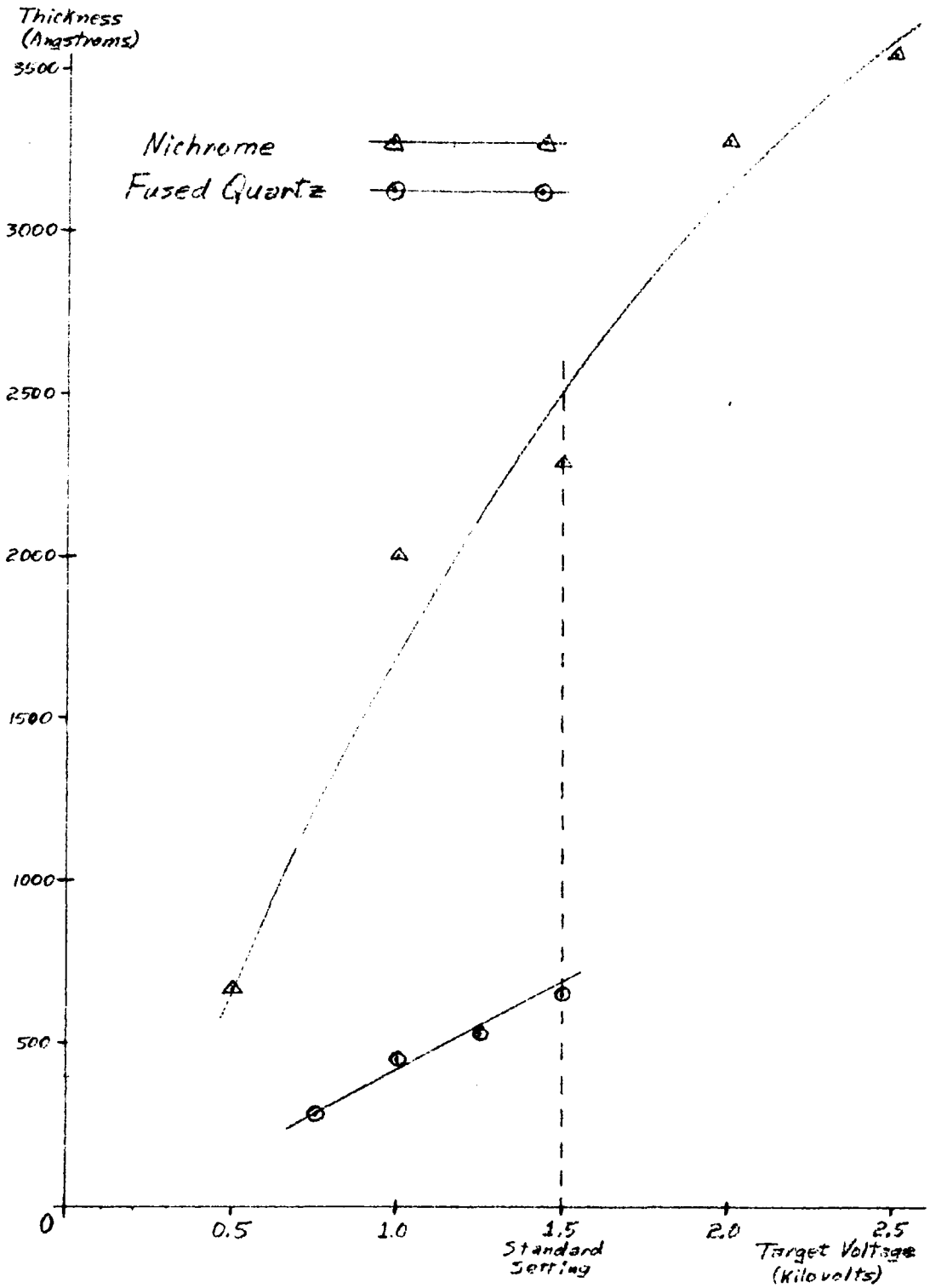


Fig. 12 Deposition Thickness vs. Target Voltage for Nichrome (D.C. voltage) and Fused Quartz (R.F. voltage)

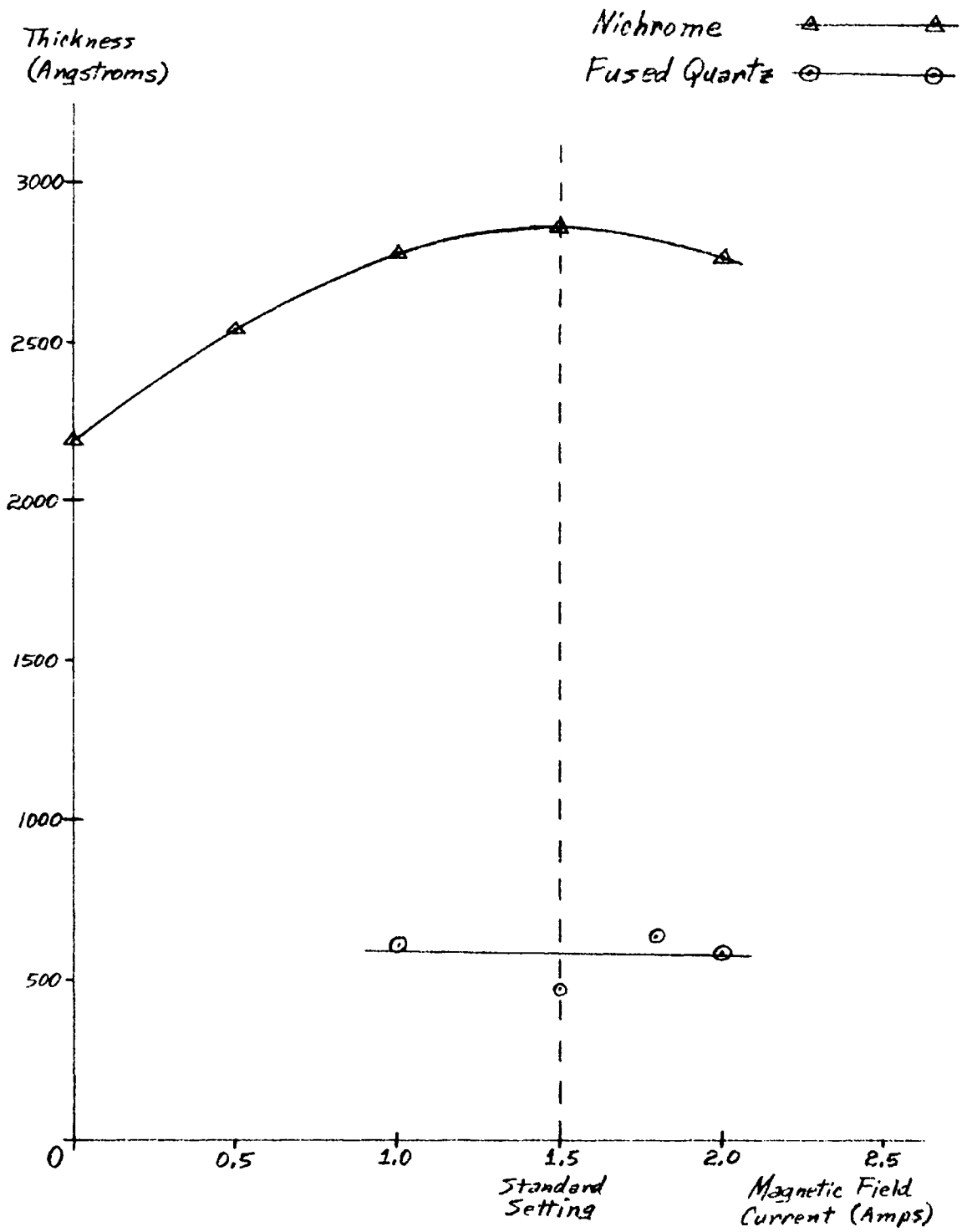


Fig. 13 Deposition Thickness vs. Magnetic Field Current for Nichrome and Fused Quartz

As the film thickness changes, the sheet resistivity of the deposited film was also noted to change. The sheet resistivity varied inversely as the thickness increased (Fig. 14). An 838 Å deposition yielded a 17 ohm/square sheet resistance for the 15 minute deposition. Subsequent depositions of 5 minutes (100 Å) and 3 minutes (less than 70 Å) yielded 70 ohm/square and 107 ohm/square sheet resistivities, respectively. Thus, for high ohm/square depositions, which are desirable for hybrid resistors, very thin nichrome films are required.

Since the nichrome films may be used for various purposes, parameter values for both maximizing and minimizing deposition rates are given. By minimizing the deposition rate, better control over the deposition of the film is obtained and reproducibility should be improved.

For maximum deposition rate the following parameter values are suggested:

1. pressure (minimum) - 2×10^{-4} torr
2. anode current (maximum) - 2.5 amperes for depositions of less than 30 minutes, 2.0 amperes otherwise. (Note: a 30 minute limit was used for 2.5 amperes because of apparent overheating of power supply components.)
3. target voltage (maximum) - 2.5 kilovolts
4. magnetic field current - 1.6 amperes
5. initial substrate temperature - 30°C and allow substrate to rise in temperature with the deposition.

To minimize the deposition rate the following parameters are suggested:

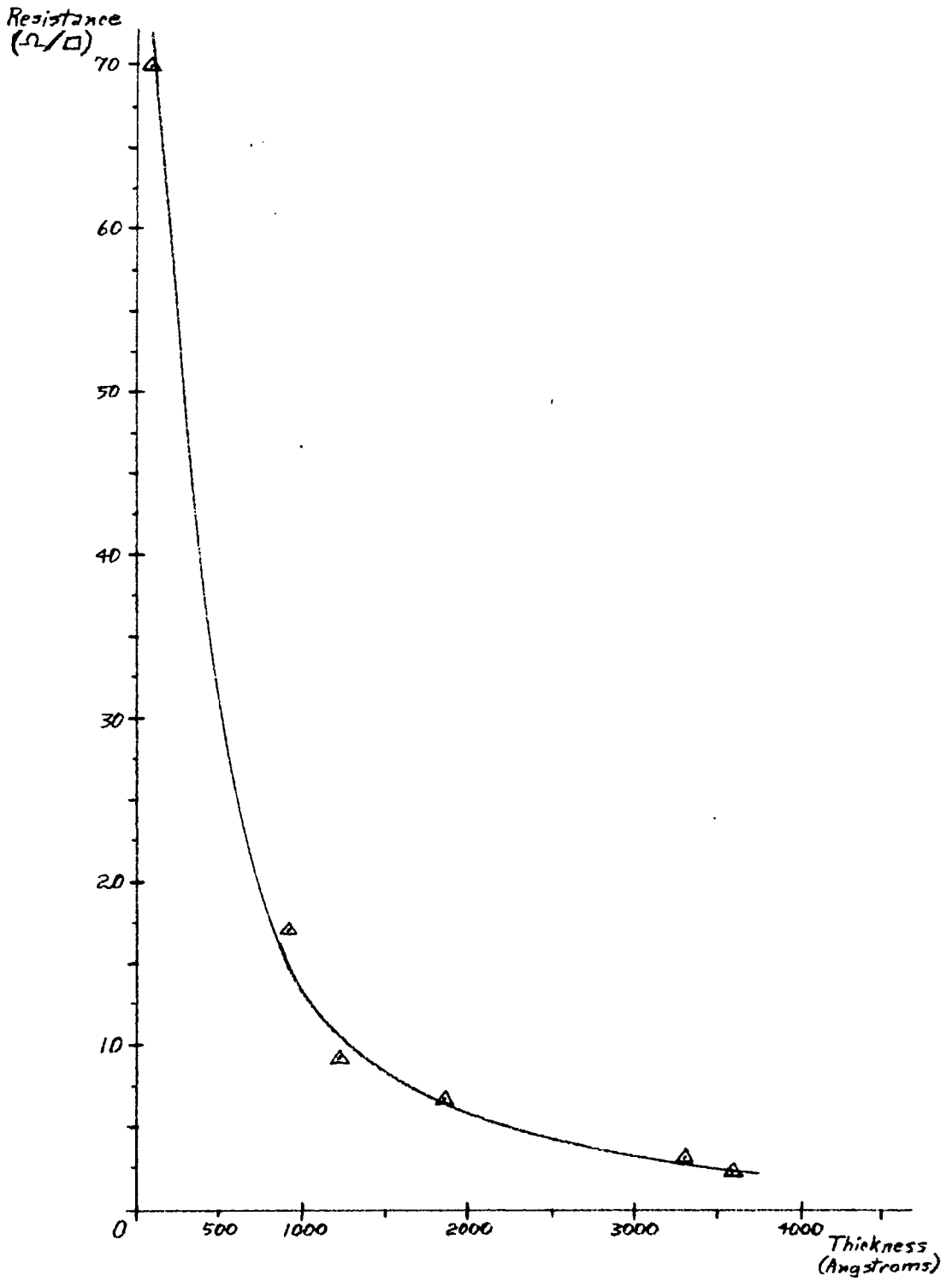


Fig. 14 Ohms/Square Resistance vs. Thickness for Nichrome

1. pressure (maximum) - 2×10^{-3} torr
2. anode current (minimum) - 0.5 amperes
3. target voltage (minimum) - 500 volts
4. magnetic field current - none
5. initial substrate temperature - 30°C

Fused Quartz Results

The results of sputter fused quartz (SiO_2) are presented next. The limits used for each variable were the same as those used for sputtering nichrome with the exception of the target voltage. Since RF biasing of the target was used for sputtering, different values were necessary for target voltage. Since repeating the other standard settings would be redundant, they are omitted from this section.

As the first parameter, time was varied and the resulting thicknesses changed in a nearly linear manner (Fig. 9). A slightly higher rate of $14.5 \text{ \AA}/\text{minute}$ was reached at 75 minutes than the $11.0 \text{ \AA}/\text{minute}$ rate at 15 minutes. Since fused quartz is already oxidized silicon (SiO_2), this change was probably due to impurities trapped on the surface of the quartz during atmospheric exposure. During this and the remaining parameter changes, the standard setting for RF target voltage was 1500 volts. The other parameters were maintained on the standard settings as noted in the section on nichrome.

Increasing the second parameter, pressure, caused slightly reduced sputtering rates (Fig. 10). But the decrease was not as noticeable as with nichrome. Again the standard settings used were the same

as for nichrome except for RF target voltage which was maintained at 1500 volts.

Changes in deposition thickness due to changing anode current were next noted. As the anode current increased, the deposition rate reached a maximum of 13.3 ⁰A/minute at 1.1 amperes and decreased thereafter (Fig. 11). Standard settings for the other parameters were as noted with RF target voltage being 1500 volts.

RF target voltage was the next parameter changed. Target voltage was varied between 750 volts and 1500 volts in 250 volt increments. Standard settings as noted under nichrome were used for the other parameters. As predicted, the deposition rate increased linearly with increasing target voltage (Fig. 12).

The last parameter to be changed was magnetic field current. Problems with arcing at the high voltage feedthrough prevented lowering the magnetic current below 1.0 amperes. Thus, only four points were obtained: 1.0 amps, 1.5 amps, 1.8 amps, and 2.0 amps of magnetic field current. Standard settings as noted under nichrome were used for the remaining parameters with the exception of RF target voltage which was held at 1500 volts. Increased magnetic field current resulted in slightly decreasing deposition rates (Fig. 13).

No runs were made with substrate temperature as a variable. This was because of the high voltage feedthrough arcing problems and the lack of noticeable effects produced on the other materials investigated.

Since the fused quartz sputtering rate is slow relative to that of metals, only suggested parameter values for maximizing the sputtering rate are given. These suggested values are:

1. pressure (minimum) - 2×10^{-4} torr (Note: pressure had only a small effect on sputtering rate.)
2. anode current - 1.1 amperes
3. RF target voltage (maximum) - 1.5 kilovolts
4. magnetic field current - 1.8 amperes
5. initial substrate temperature - 30°C and allow to rise as the deposition progresses.

No study of the crystalline structure due to substrate temperature changes was undertaken. The author feels such changes of temperature may change the dielectric properties of fused quartz considerably and further study of this variable would be beneficial.

Nickel, Molybdenum and Tantalum Results

The results of sputtering nickel, molybdenum and tantalum are presented together, not because they were necessarily similar, but for presentation simplicity. Once again time was the first parameter varied. The standard settings noted under nichrome were used for the remaining parameters. The tantalum and molybdenum depositions increased linearly with time (Fig. 15). The deposition rates were $30 \text{ \AA}^{\circ}/\text{minute}$ for tantalum and $37 \text{ \AA}^{\circ}/\text{minute}$ for molybdenum. This indicates that any oxides formed during atmospheric exposure sputtered at about the same rate as the pure material in these cases. The nickel deposition rate decreased with time from $49 \text{ \AA}^{\circ}/\text{minute}$ at 15 minutes to $37 \text{ \AA}^{\circ}/\text{minute}$ at 75 minutes. This indicates that oxides of nickel formed during brief atmospheric exposure sputter more readily than the pure nickel target material.

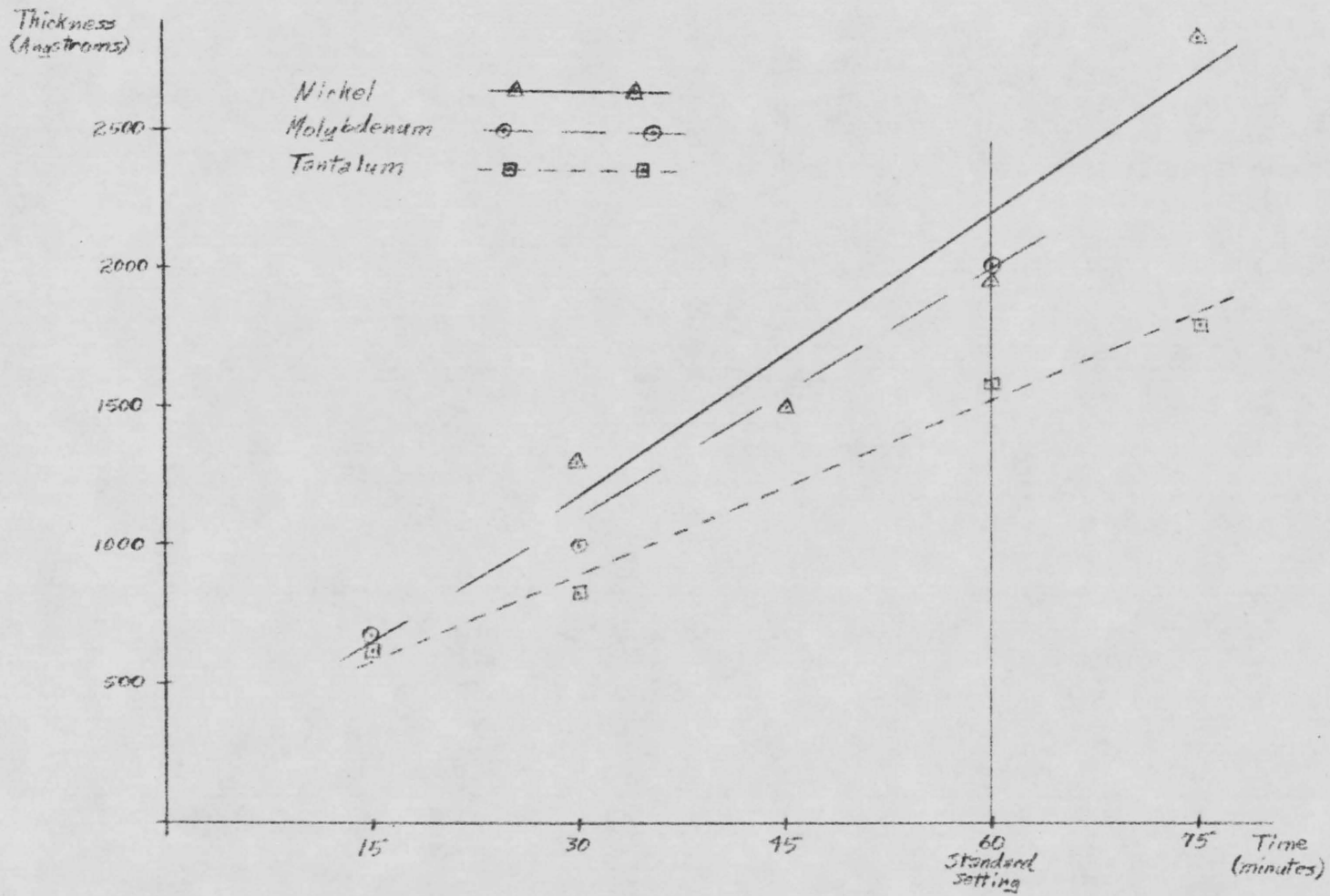


Fig. 15 Deposition Thickness vs. Time for Nickel, Molybdenum and Tantalum

The second parameter to be varied was pressure. Both the limits of variance and the remaining parameter standard settings were the same as noted for nichrome. Pressure increases had little effect on the deposition rates of nickel or tantalum (Fig. 16). Only two points were available for molybdenum and these indicated little effect on sputtering rate due to pressure changes. (Note: About half of the molybdenum depositions were very coarse and grainy in appearance with poor adhesion to the glass slide. No thickness measurements nor resistivity measurements were possible on these depositions. The remainder were very smooth and reflective and had good adhesion to the glass slides. On several depositions the reflective, highly adhesive deposition at one end of the slide gradually changed to a grainy non-adhesive deposition at the other end. This indicates that poorly cleaned slides were not the cause of the poor depositions. No experiments were pursued which might have offered an explanation of this observed film deterioration.)

Anode current was the next parameter to be varied. The standard settings and the varied parameter limits were the same as noted for nichrome. Anode current increases caused nearly linear deposition rate increases for nickel and tantalum (Fig. 17). The two available points for molybdenum suggest that its sputtering rate also increased with increasing anode current.

The next parameter to be varied was target voltage. Standard settings of the other parameters were also the same as for nichrome. As the target voltage increased, the deposition rates also rose nearly linearly for nickel, molybdenum and tantalum (Fig. 18).

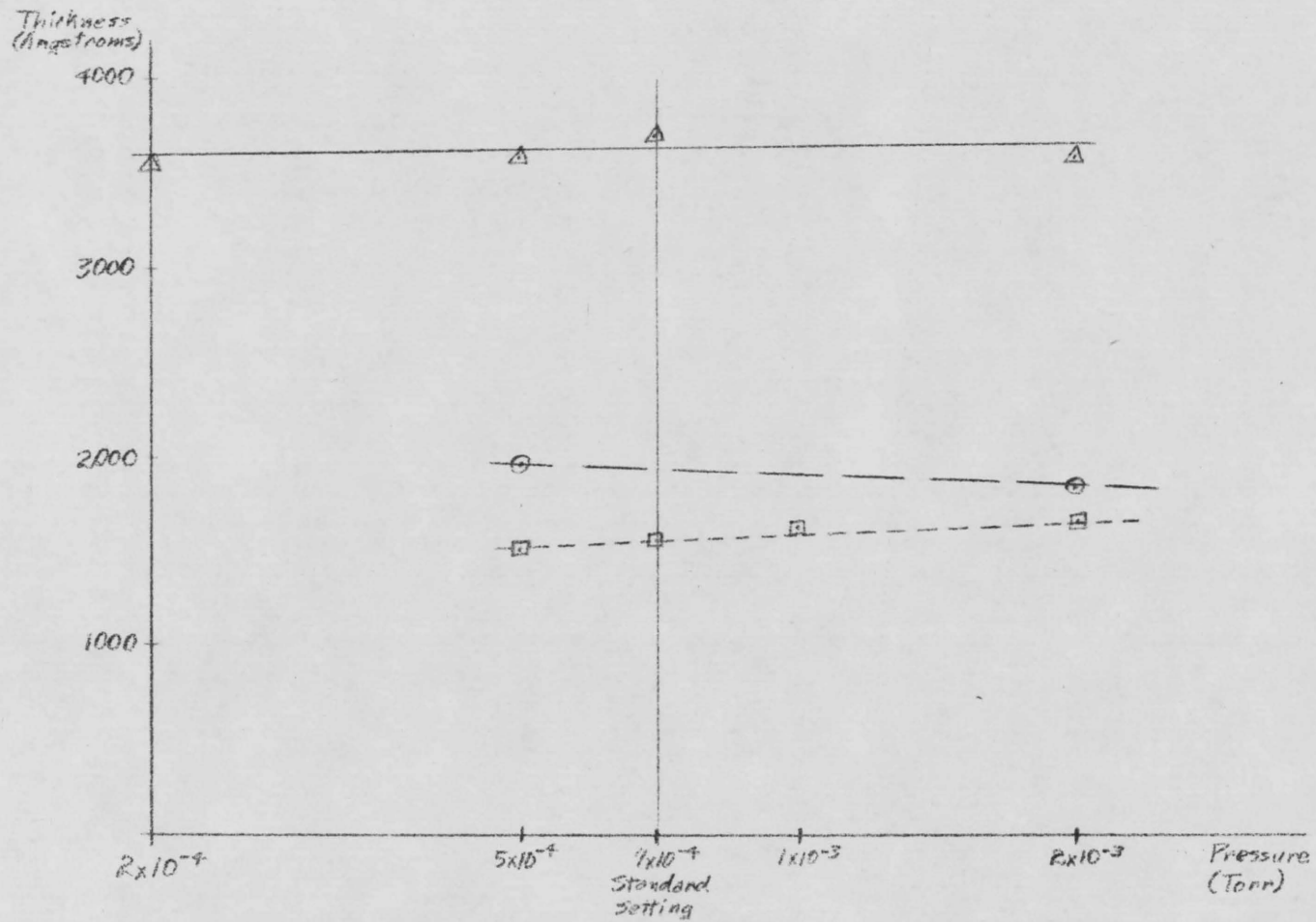


Fig. 16 Deposition Thickness vs. Pressure for Nickel, Molybdenum and Tantalum

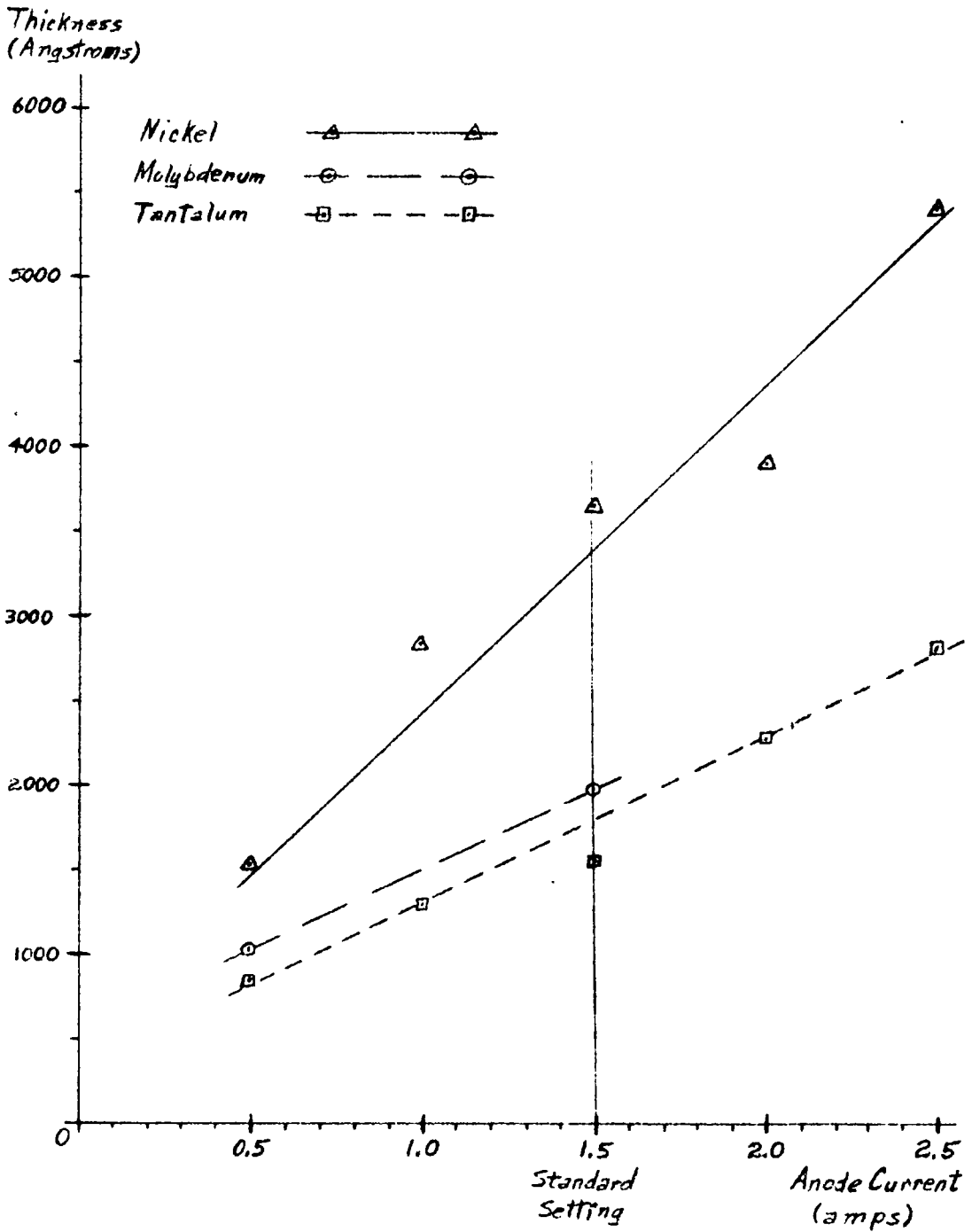


Fig. 17 Deposition Thickness vs. Anode Current for Nickel, Molybdenum and Tantalum

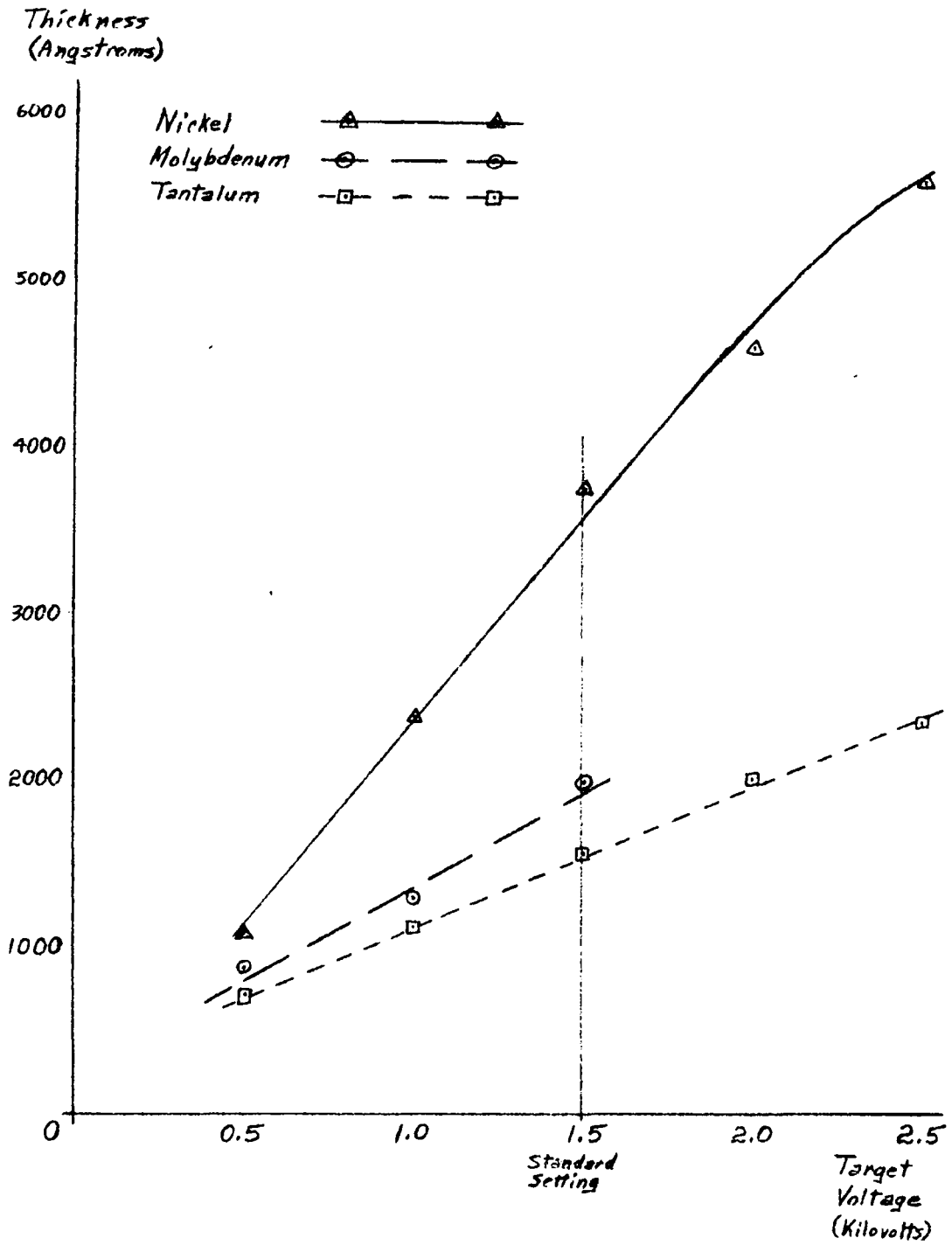


Fig. 18 Deposition Thickness vs. Target Voltage for Nickel, Molybdenum and Tantalum

Magnetic field intensity as indicated by magnetic field coil current was the next parameter varied. The same limits as for nichrome were used and the same standard settings as for nichrome were used for the other parameters. For nickel the deposition rate increased with increasing magnetic field current (Fig. 19). The rate appeared to approach a maximum value which was beyond the largest value attainable with the current available from the control console. The tantalum deposition rate was greatest for no magnetic field current (Fig. 19). No results were obtained for the molybdenum as magnetic field current was varied.

The last parameter varied was substrate temperature. As mentioned earlier the results of varying substrate temperature were inconclusive for nickel and tantalum. No results were obtained for molybdenum.

Sheet resistance measurements provided an indication of how useful the different thicknesses of film may be for hybrid resistor fabrication. The sheet resistance of nickel increased as the inverse of the deposition thickness (Fig. 20). A film of 5500\AA had only 0.25 ohm/square resistance while that for 1100\AA had 2 ohm/square. Such low values of sheet resistance indicate the usefulness of nickel would be limited for hybrid resistor fabrication. In order to raise the sheet resistance, undesirably thin films would be necessary. Molybdenum sheet resistances were higher than that of nickel but were also impractically low for hybrid resistor fabrication (Fig. 20). A 1920\AA molybdenum film had a sheet resistance of 3.2 ohm/square while an 820\AA deposition had only a 14 ohm/square sheet resistance. The sheet resistance of molybdenum also

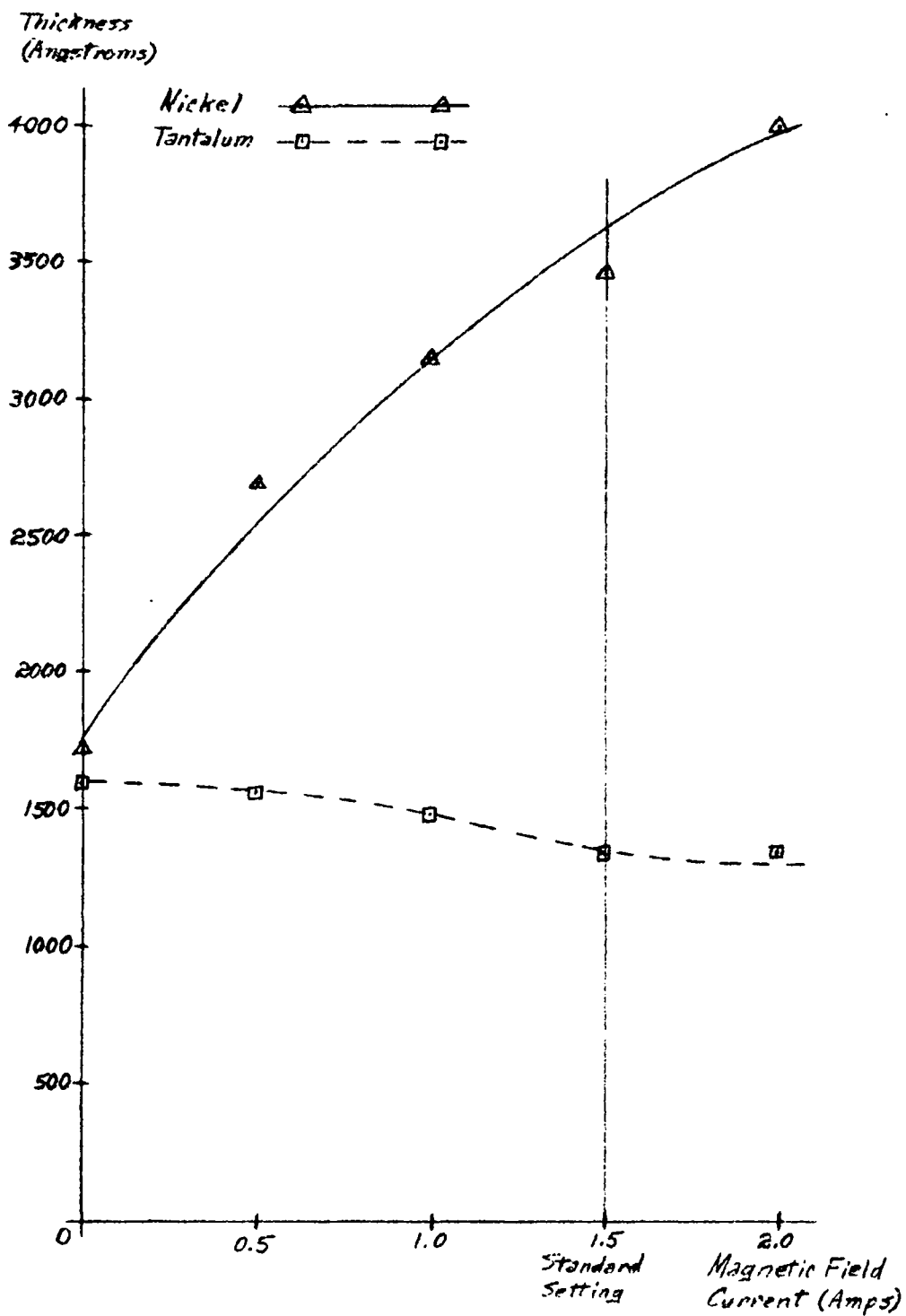


Fig. 19 Deposition Thickness vs. Magnetic Field Current for Nickel and Tantalum

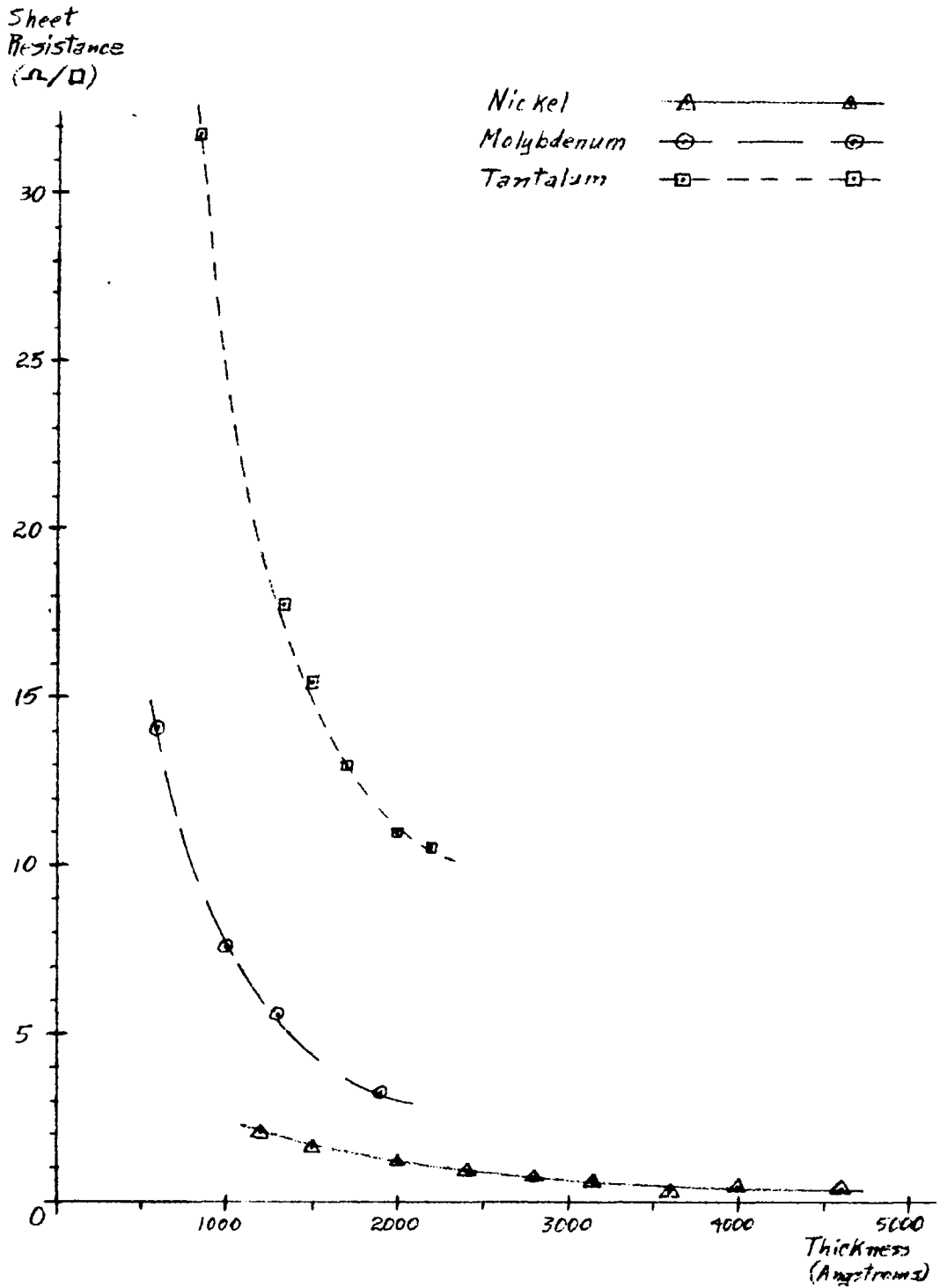


Fig. 20 Sheet Resistance vs. Thickness for Nickel, Molybdenum and Tantalum

increased with the inverse of deposition thickness. Sheet resistance for tantalum increased as the inverse of deposition thickness (Fig. 20). Although the sheet resistance was much higher, 16 ohm/square for a 1500^oÅ deposition, there was also a large variation in the sheet resistance values for approximately equal thickness depositions. The initial reaction that tantalum would make a good hybrid resistor metal is thus tempered by realizing the problem of reproducibility. Furthermore, processing of the tantalum films into resistors is difficult as is explained more fully in the next section. The literature indicated that the resistance of tantalum films is highly dependent upon the amount of oxide present in the film (see Chapter 2). No precise control of the oxygen partial pressure was available in the vacuum system-sputtering module used for these experiments. A gas analyzer would be necessary to monitor the oxygen content of the module if consistent control of the oxygen partial pressure were to be undertaken. No such equipment was available for use in the Solid State Engineering Laboratory.

The choice of parameters to maximize the sputtering rates of nickel and tantalum are the same as given below:

1. pressure - 1×10^{-3} torr (maximum allowed to maintain mean free path greater than target-substrate distance.)
2. anode current (maximum) - 2.5 amperes for depositions of less than 30 minutes, 2.0 amperes otherwise
3. target voltage (maximum) - 2.5 kilovolts
4. magnetic field current (maximum) - 2.0 amperes
5. initial substrate temperature - 30^oC

The parameters for maximizing the molybdenum sputtering rate are slightly different as indicated below:

1. pressure - not enough results obtained for conclusive recommendations but would use 7×10^{-4} torr
2. anode current (maximum) - 2.5 amperes for depositions of less than 30 minutes, 2.0 amperes otherwise
3. target voltage - 2.5 kilovolts
4. magnetic field current - no results obtained
5. substrate temperature - no results obtained

General Observation

The following general observations are made on the results produced by changing each of the sputtering parameters:

1. The deposition rates of all the materials remained reasonably constant as time increased once surface oxides and contamination was removed. This was as expected. Surface oxides and contamination were generally removed within the first fifteen minutes of sputtering. The effects of these oxides and contaminants on deposited films are undesirable and unpredictable. Since short sputtering times are required for hybrid resistor application of the metals investigated, some method of masking the substrate during the initial sputtering period would be desirable. An internal shutter mechanism would be the most practical method but may be impractical in the present R. D. Mathis module.
2. Only nichrome showed a large reduction in sputtering rate as pressure increased. Tantalum and nickel showed slight increases

while fused quartz showed a slight decrease in sputtering rate.

3. All but fused quartz showed large nearly linear increases in sputtering rate as anode current increased.

4. Target voltage increases resulted in faster sputtering rates for all materials studied.

5. Increasing magnetic field current produced a maximum sputtering rate for nichrome and an increased sputtering rate for nickel. Presence of any magnetic field caused a slight decrease in sputtering rate for tantalum.

6. Sheet resistance varied inversely with the deposition thickness for all the metals investigated. Such a variation is expected since sheet resistivity (R_s) is inversely proportional to the thickness (X):

$$R_s = \frac{\bar{\rho}}{X}$$

where $\bar{\rho}$ is the uniform resistivity of the sample.

Processing Compatibility

To be useful thin films for hybrid resistors must permit processing techniques compatible with bipolar active devices protected only by a silicon dioxide layer. Compatible processes must provide proper adhesion to silicon dioxide as well as allow shaping of resistors by normal photoresist etching techniques. Not all of the metals investigated provided this compatibility. Nichrome and nickel possessed the highest degree of process compatibility. Both adhered well to silicon dioxide once moisture had been reduced by baking. Both were readily etched with

a dilute HCl-HNO_3 acid solution which would not attack the silicon dioxide. Process compatibility of molybdenum was somewhat less, as adhesion to silicon dioxide was poor on about half of the depositions. Compatible etching was provided by a dilute $\text{H}_2\text{SO}_4\text{-HNO}_3$ mixture which readily etched molybdenum but would not attack silicon dioxide. No compatible method of etching tantalum was found. Dilute HF acid was found to be the only etch for tantalum and this etches silicon dioxide also. Furthermore, photoresists would not adhere to tantalum so the only method available to form tantalum resistors was mechanical masking.

Since nichrome appeared to have higher sheet resistance and at least equal process compatibility with nickel, it was chosen for the processing of hybrid resistors. The results of the study of sputtered hybrid resistor and resistor-capacitors is presented in the next chapter.

Chapter 5

HYBRID RESISTOR AND CAPACITOR FABRICATION RESULTS

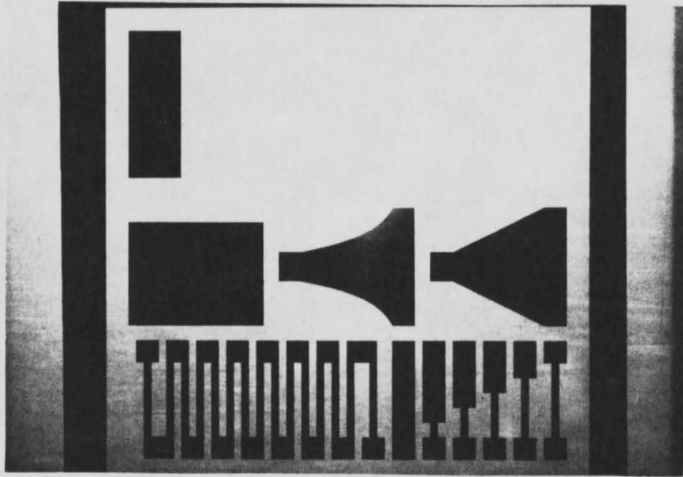
The ultimate objective of sputtering thin films is to make useful hybrid resistors and capacitors for microcircuits. This chapter is prefaced by a section indicating the desired range of values for resistors and capacitors followed by a description of the evaluation pattern used. The next section presents the expected and measured values of the resistors fabricated by sputtered films. Comments on reproducibility experienced and problems encountered are included in this section. The last section presents the theoretical values of capacitors expected and the test results of the capacitors realized. Evaluation of capacitor fabrication problems is also given in this section.

The goal when making hybrid thin film resistors is to provide a greater range of resistor values, particularly high values, which are difficult to obtain using diffused resistor techniques. The desired range of resistance values is from several hundred ohms to several hundred thousand ohms. Since hybrid resistors can be placed on top of any part of the silicon dioxide covered substrate, except in contact areas, folded resistors of 100 mil lengths are possible on a 60 x 60 mil square die. For a 200k ohm resistor, the sheet resistivity of the thin film would have to be 2000 ohm/sq. At the lower extreme, a resistance on the order of 200 ohms with a 5 mil length requires a sheet resistance of 40 ohms/sq. Thus, the desired range of film sheet resistance is 40

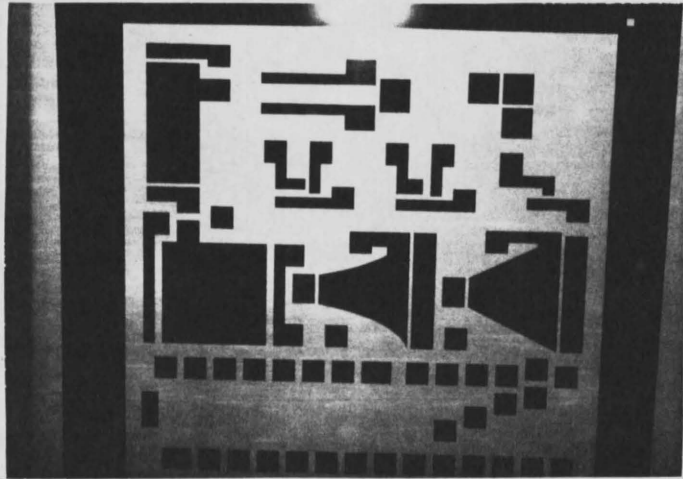
ohm/sq. to 2000 ohm/sq. This will provide a resistor range from 200 ohm to 200k ohms.

The goal in making hybrid thin film capacitors is to maximize the capacitance value obtained while minimizing the area required. To maintain a sufficiently high breakdown voltage for general circuit design, a rather severe limitation is placed on thin film capacitors. Since the dielectric thickness determines the breakdown voltage for any given material, only the area can be changed to alter the capacitor value for any particular material. A breakdown voltage of 5 volts requires a SiO_2 dielectric thickness of 500 \AA . With a dielectric thickness of 500 \AA , 10×10 mil capacitance will have a value of about 5.5 pfd. In a similar manner, for a 5 volt breakdown voltage only 500 \AA dielectric thickness is required. In this case a 10×10 mil capacitance would have a 55 pfd value. Thus, even for low breakdown voltage, relatively large areas are required to obtain even moderately small size capacitors. The primary advantage of hybrid film capacitors is their low leakage currents and voltage independent values.

In order to evaluate the resistors and capacitors a versatile evaluation pattern was required. The pattern decided upon contained nine 1 mil dogbone resistors varying from 2 mils to 10 mils in length (Fig. 21a). The wide contact area at one end of each of these resistors was extended to form 3 mil wide resistors varying from 2 mils to 10 mils in length. A 150 mil folded 1 mil wide resistor was provided with probe points at each fold, i.e., every 10 mils along its length. Two tapered resistors were provided which were to be used as distributed



(a)



(b)

Fig. 21 Mask

element resistors in a notch filter design (Fig. 21b). Two large area rectangular resistors were also provided to serve as distributed element non-tapered resistors in a resistor-capacitance combination. The remaining area was left available for making connections to diffused devices in the substrate. For example, active diffused devices could be connected to distributed resistor-capacitance elements to form a hybrid notch filter design.

Resistor Results

Using the film thickness measurements and sheet resistance measurements of the preceding chapter, the following theoretical values are calculated for the resistors of the evaluation pattern. A three minute deposition of less than 70 \AA thickness produced a thin film with sheet resistivity of 110 ohm/sq . Thus a $1 \times 10 \text{ mil}$ dogbone resistor should have a resistance of 1.1k ohms for this thickness. The actual values measured on different die on the same wafer for this resistor and deposition varied from 1.04k ohms to 1.8k ohms . The $3 \times 10 \text{ mil}$ resistor has a theoretical value of 366 ohm and measured values varying from 333 ohms to 900 ohms on different die of the same wafer. The reason for this spread can be attributed to varied undercutting of the photoresist during etching. This caused some resistors to be less than their prescribed 1 or 3 mils width and others to remain very close to the 1 or 3 mils desired size.

The larger tapered and rectangular resistors had similar results. The thin rectangular resistor has a theoretical value of 314 ohms based on 110 ohm/sq . sheet resistance. The observed values of several die on

one wafer varied from 1k ohm to 3k ohms but on another, they only varied from 600 ohms to 750 ohms.

The linear tapered resistor has a theoretical value of 132 ohms using 110 ohm/sq. sheet resistivity. But actual probed values varied from 375 ohms to 504 ohms. The probable cause for these much higher than calculated values is that the probes were causing current crowding near the point of contact. This would decrease the effective resistor width at both ends and make the resistance appear higher than the theoretical value. To obtain more accurate measurements, thick aluminum contacts should be evaporated over the contact areas to use for connections. This would also minimize damage to the resistors due to probing and provide nearly equipotential ends for the tapered and rectangular resistors.

Capacitor Results

The results of two wafers of capacitors were poor. Dielectric shorts prevented measurement of any capacitance values. This was probably due to pinholes caused by dust present in the working area of the sputtering module. Theoretically a one hour 800\AA ⁰ thick sputtered fused quartz deposition should produce a value of about 60 pfd for the large rectangular capacitor with a breakdown voltage of 8 volts. The linear taper should have a capacitance of 41 pfd and a breakdown voltage of 8 volts.

Since all of the capacitors tested were shorted, no notch filter results were obtained. But once the technical problems associated with making capacitors are overcome, making a distributed element notch filter should follow fairly easily.

Chapter 6

CONCLUSIONS

The primary goal stated in Chapter 1 for this thesis and its associated experimental work was to characterize the R. D. Mathis sputtering module for several different materials. A secondary goal was to make useful hybrid resistors and distributed element resistor-capacitors, and to use these resistor-capacitors to make a simple notch filter.

The primary goal was successfully realized. From the graphs of Chapter 4, one can determine the parameter values necessary to obtain thin films having a wide range of sheet resistances. Values for maximizing sputtering rates are suggested. Values for minimizing nichrome sputtering rate are given. By choosing the proper values for each parameter from the graphs of Chapter 4 the sputtering rate of each of the other materials can also be minimized.

The secondary goal of producing usable hybrid resistors and capacitors was partially realized. Hybrid resistors of various values were obtained as presented in Chapter 5. The distributed element resistor-capacitors were formed and the distributed resistor part of the resistor-capacitors had approximately the anticipated values. However, all of the capacitors had dielectric short circuits. Dust-caused pinhole shorts are suspected of being the source of these

short circuits. Further refinement of process cleanliness and development of pinhole evaluation methods will be necessary to eliminate this problem.

Without capacitances, notch filter evaluations could not be completed. Once capacitors are realized, the notch filter using an external amplifier should be easily realized. Use of diffused device amplifiers fabricated in the substrate will result in hybrid microminiaturization.

Appendix A

SPUTTERED THIN FILM DEPOSITION PROCEDURE

The following steps were taken during each sputtering deposition run starting with the sputtering module open:

1. locate substrate(s) as desired on substrate platform
2. close vacuum system by lowering and seating module on base ring

3. pump down to less than 10^{-6} torr

(a) for resistor depositions only, heat substrate to 150°C for 20 minutes followed by 200°C for 5 minutes then allow to cool to about 50°C before deposition.

4. set filament at 6.4 amperes
5. set magnetic field current at 1.8 amperes
6. set anode current control to vertical position

(Note: no current flow will be indicated on meter until plasma is formed.)

7. backfill with argon to about 7×10^{-4} torr using micrometer needle valve

8. increase filament current until plasma forms
9. return filament current to 6.4 amperes
10. set anode current to 1.5 amperes
11. allow ion scrubbing to proceed for 5 minutes
12. raise target voltage to desired voltage
13. set all parameters to desired values

14. let sputtering run continue for desired time
15. turn off target voltage
16. turn off anode current
17. turn off filament current
18. turn off magnetic field current
19. close micrometer needle valve
20. return vacuum system to atmospheric pressure; vent with dry nitrogen when appropriate
21. raise sputtering module and remove substrates.

Appendix B

ETCHING PROCEDURES

In order to determine the sputtering rate as each control parameter was varied, two quantities are necessary: time and deposition thickness. Time is readily measured but deposition thickness is not so easily measured. In order to use the Reichert microscope for thickness measurements, adjacent reflective surfaces from the top of the deposition and from the substrate material are necessary (Fig. 22a). The most practical method for obtaining the reflective step was to first etch a channel through the deposited material to the substrate material and then evaporate a uniform aluminum reflective film over the entire substrate (Fig. 22b). The etching process to be described was also used in processing the thin film resistors and capacitors from the deposited materials.

The etching process used was:

1. Dry the substrate with deposited film for 10 minutes at 110°C . This step is unnecessary if the film is just removed from the sputtering module.
2. Apply photoresist.
 - a. Apply KPR to glass slides by eyedropper; allow the film to form over the entire face of the slide. Allow KPR to drain standing the slide on end for at least 10 minutes.

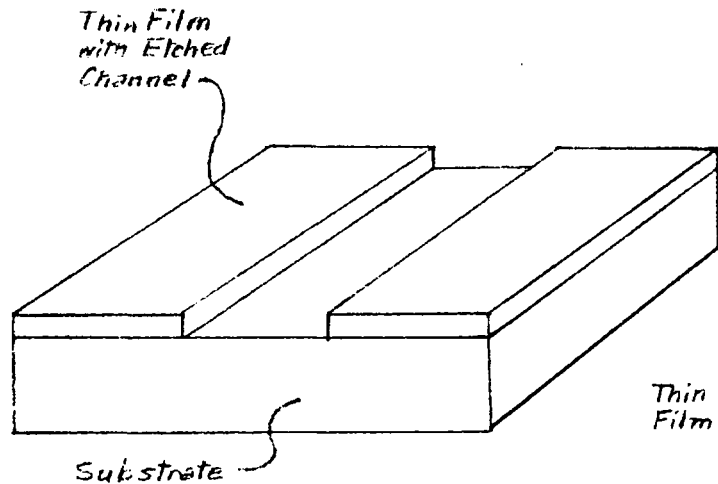


Fig. 22a Thin Film on Substrate with Etched Channel

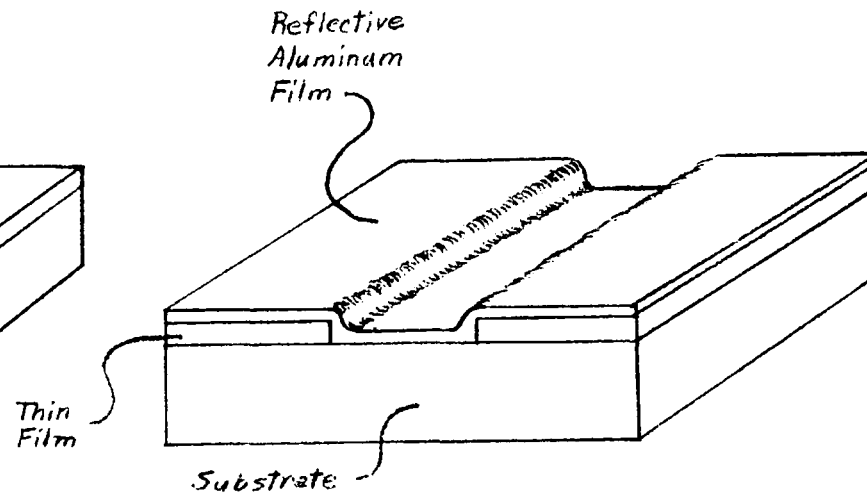


Fig. 22b Thin Film on Substrate with Reflective Aluminum Film for Thickness Measurements

b. Apply KPR to wafers with eyedropper covering entire wafer. Spin for 10 seconds at 2000 rpm.

c. Apply KMER to wafers with sputtered SiO_2 with an eyedropper. Spin for 10 seconds at 10,000 rpm.

3. Prebake for 15 minutes at 110°C .

4. Expose

a. Expose KPR under large overhead fixture for 2 minutes, or

b. expose KPR under K & R mask alignment fixture for 6 seconds, or

c. expose KMER under old mask alignment fixture for 15 seconds.

5. Develop

a. Develop KPR in KPR developer for 1 minute, or

b. develop KMER in KMER developer for 15 seconds.

6. Wash in isopropyl alcohol and blow dry with dry nitrogen.

7. Postbake

a. Postbake KPR for 15 minutes at 110°C , or

b. postbake KMER for 20 minutes at 160°C .

8. Etch

a. Etch nickel and nichrome in hot (about 65°C) dilute HNO_3 and HCl mixture (by volume 1 part HNO_3 and 1 part HCl and 2 parts H_2O) for 5 to 10 seconds.

b. Etch molybdenum in hot (about 65°C) dilute HNO_3 and H_2SO_4 mixture (by volume 1 part HNO_3 and 1 part H_2SO_4 and 3 parts H_2O) for 5 to 10 seconds.

c. Etch tantalum on silicon only in dilute HF (by volume 1 part 49% HF and 3 parts H_2O) for about 20 seconds.

d. Etch silicon dioxide in buffered HF (by volume 1 part 49% HF and 4 parts NH_4F) for about 3 minutes.

9. Remove exposed photoresist

a. Remove exposed KPR by placing in hot (about 80°C) trichlorethylene (TCE) for 20 to 30 minutes then spray with TCE. Wash in isopropyl alcohol and dry with dry nitrogen. Inspect for photoresist remaining and repeat this step until all photoresist is removed.

b. Remove exposed KMER by immersing in hot H_2SO_4 for 5 minutes. Wash in H_2O then in isopropyl alcohol and dry with dry nitrogen. Inspect and repeat if necessary.

For thickness measurements place wafer in vacuum evaporative system and evaporate about $1000\overset{\circ}{\text{A}}$ of reflective aluminum over the step area. Measure thickness using Reichert microscope with Nomarski polarization interferometer attached.

REFERENCES

- Blevis, Earl H., "Glow Discharge Sputtering-Theory and Practice", distributed by R. D. Mathis Co., 1345 Gaylord St., Long Beach, Calif., 90813, Feb. 1964.
- Hall, John, "Sputtered Microcircuits, From the Laboratory to Production," from the Second Symposium on the Deposition of Thin Films by Sputtering, June 6-7, 1967.
- Moore, G. E., "Dissociation of Absorbed CO by Slow Electrons," Journal of Applied Physics, Vol. 32, No. 7, p. 1241, July 1961.
- Nickerson, John W. and Roger Moseson, "Application of Low Energy Sputtering for Thin Film Deposition," reprinted from Semiconductor Products - Solid State Technology, Dec. 1964, by Consolidated Vacuum Corp.
- Nickerson, John W. and Roger Moseson, "Low-Energy Sputtering," reprinted from Research/Development, March 1965, by Consolidated Vacuum Corp.
- Peterman, L. A., "Gas Desorption Efficiency under Electron Bombardment," Nuovo Cimento (Italy) Ser. 1, Vol. 1, No. 2, pp. 601-11, 1963. [Presented at Residual Gases in Electron Tubes Symposium, Milan, 1963.]
- Redhead, P. A., "Interaction of Slow Electrons with Chemisorbed Oxygen," Canadian Journal of Physics, Vol. 42, No. 5, p. 886, May 1964.
- Seeman, James M., "Bias Sputtering: Its Techniques and Applications," from Symposium on Deposition of Thin Films by Sputtering, June 1966.
- Seeman, James M., "Ion-sputtered Thin Films," from a paper presented at the Sixth Annual Structures and Materials Conference of the American Institute of Aeronautics and Astronautics, 5-7 April 1965, Palm Springs, Calif.
- Vratny, F. and D. J. Harrington, "Tantalum Films Deposited by Asymmetric A-C Sputtering," Journal of the Electrochemical Society, pp. 484-489, Vol. 112, No. 5, May 1965.
- Wolsky, S. P., "Sputtering Processes and Film Depositions," presented at Symposium on the Deposition of Thin Films by Sputtering on June 9, 1966.